SPECIAL FEATURE

Metapopulations, the Inflationary Effect, and Consequences for Public Health

Nicholas Kortessis,[1,*] Gregory Glass,[2,3] Andrew Gonzalez,[4] Nick W. Ruktanonchai,[5] Margaret W. Simon,[6] Burton Singer,[3] and Robert D. Holt[6]

1. Department of Biology, Wake Forest University, Winston-Salem, North Carolina 27106; 2. Department of Geography, University of Florida, Gainesville, Florida 32611; 3. Emerging Pathogens Institute, University of Florida, Gainesville, Florida 32610; 4. Department of Biology, McGill University, Quebec H3A 1B1, Canada; 5. Department of Population Health Sciences, Virginia Polytechnic University, Blacksburg, Virginia 24061; 6. Department of Biology, University of Florida, Gainesville, Florida 32611

Submitted November 4, 2023; Accepted October 22, 2024; Electronically published January 3, 2025

Online enhancements: supplemental PDF.

ABSTRACT: The metapopulation concept offers significant explanatory power in ecology and evolutionary biology. Metapopulations, a set of spatially distributed populations linked by dispersal, and their community and ecosystem level analogs, metacommunity and metaecosystem models, tend to be more stable regionally than locally. This fact is largely attributable to the interplay of spatiotemporal heterogeneity and dispersal (the inflationary effect). We highlight this underappreciated (but essential) role of spatiotemporal heterogeneity in metapopulation biology, present a novel expression for quantifying and defining the inflationary effect, and provide a mechanistic interpretation of how it arises and impacts population growth and abundance. We illustrate the effect with examples from infectious disease dynamics, including the hypothesis that policy decisions made during the COVID-19 pandemic generated spatiotemporal heterogeneity that enhanced the spread of disease. We finish by noting how spatiotemporal heterogeneity generates emergent population processes at large scales across many topics in the history of ecology, as diverse as natural enemy–victim dynamics, species coexistence, and conservation biology. Embracing the complexity of spatiotemporal heterogeneity is vital for future research on the persistence of populations.

Keywords: spatiotemporal heterogeneity, persistence, asynchrony, source-sink dynamics, dispersal, natural enemy–victim interactions.

Introduction

The concept of a metapopulation—a set of spatially distributed populations linked by dispersal—is central to discourse in ecology, evolution, and conservation biology. Metapopulation theory (Hanski and Gaggiotti 2004) and its community-level counterpart, metacommunity theory (Leibold et al. 2022), address important issues in ecology, including population persistence (Levins 1969), species coexistence (Amarasekare 2003; Hoopes et al. 2005), community assembly (Thompson and Gonzalez 2017; Leibold et al. 2022), and community stability (Loreau et al. 2003; Thompson et al. 2017). Metapopulation models help advance understanding of biogeographic patterns (Gonzalez et al. 1998) and evolutionary processes, such as the ecology and evolution of range limits (Holt and Keitt 2000), the evolution of dispersal (Olivieri et al. 1995; Wang and Altermatt 2019), and the interplay of selection and gene flow in adaptive evolution and evolutionary rescue (Ingvarsson 2002; Bell and Gonzalez 2011; Hanski et al. 2011). In applied contexts, metapopulation perspectives pertain to biocontrol (Levins 1969) and analyses of habitat loss and fragmentation (Ovaskainen and Hanski 2004). Here, we bring out the sometimes hidden theme of spatiotemporal heterogeneity as a key driver of metapopulation processes.

Metapopulation theory emerged from observations by empirical ecologists—such as Andrewartha and Birch (1954), Huffaker (1958), and den Boer (1968)—on the often ephemeral and unstable nature of local populations. The formal theory, stemming back to the seminal paper of Levins (1969) for a single species (the term "metapopulation" had its first usage in Levins [1970]), addresses the challenge of understanding the interplay of dispersal and complex temporal and spatial environmental heterogeneities. Levins's (1969) original metapopulation model described a set of spatially discrete extinction-prone local populations connected

* Corresponding author; email: kortessn@wfu.edu.

ORCIDs: Kortessis, https://orcid.org/0000-0003-4690-7508; Glass, https://orcid.org/0000-0002-8560-2451; Gonzalez, https://orcid.org/0000-0001-6075-8081; Ruktanonchai, https://orcid.org/0000-0001-6500-7121; Simon, https://orcid.org/0000-0001-8269-2589; Singer, https://orcid.org/0000-0002-5295-5971; Holt, https://orcid.org/0000-0002-6685-547X.

 https://doi.org/10.1086/733896

by dispersal. In this model, he assumed (1) that individuals move equally between all populations, (2) that the dynamic nature of local environments and population growth cause local extinctions, occurring independently across populations; and (3) that extinctions and colonization events were slow compared with local population dynamics. From this model, Levins derived conditions for the persistence of an agricultural pest and the efficacy of different control strategies.

Today, the term metapopulation is used more expansively than originally defined by Levins. It describes a region spanning multiple local populations where the dynamics of local populations are determined by local processes and movement among local populations (i.e., emigration and immigration). The metapopulation idea has been expanded to include multiple species and their interactions (Wilson 1992) in what are called metacommunities, that is, spatially distributed sets of multispecies communities, with extinction and colonization events determining ecological and evolutionary patterns and processes both locally and regionally (Hoopes et al. 2005).

Like all valuable theory, metapopulation and metacommunity theories neglect many complexities of the world to make other complexities manageable. A full accounting of population dynamics in space, even without intrinsic spatial and temporal environmental heterogeneities, leads to challenging mathematical problems (Holmes et al. 1994; see, e.g., Bolker and Pacala 1997). Metapopulation and metacommunity theories simplify space into suitable habitat patches surrounded by nonhabitat, akin to islands in an ocean. This maps well to some naturally patchy ecosystems (such as ponds, specialist host plants, and agricultural fields that motivated Levins's original model), but this abstraction also makes other spatial problems tractable. Some models track presence or absence, which we call "occupancy models." In such models, changes in occupancy reflect local extinction and colonization events. Others track local population densities, which we call "patch models." In these models, changes in density reflect demographic processes (birth, death, and movement). Occupancy and patch models are complementary frameworks, each with strengths and limitations, and the differing assumptions made in each framework provide complementary insights into spatially distributed population and community dynamics at large scales.

The simplifying assumptions of metapopulation models sometimes mask critical processes important to their dynamics. Here, we look under the hood of classical metapopulation occupancy models to bring out—and make explicit—key but largely unrecognized assumptions crucial to their behavior. The major implicit assumption we wish to highlight is the presence of spatiotemporal heterogeneity in occupancy models. First, we reflect on how occupancy models of metapopulations and metacommunities embody spatiotemporal heterogeneity. Without spatiotemporal heterogeneity, many predictions from classical metapopulation and metacommunity theories no longer hold. Second, we explore a phenomenon that has received attention in the theoretical literature but comparatively little empirical exploration—the "inflationary effect" (a term coined in Gonzalez and Holt 2002). The inflationary effect is the elevated average growth (Kortessis et al. 2020) or average abundances (Gonzalez et al. 1998) emerging in spatiotemporally heterogeneous landscapes coupled by dispersal compared with landscapes without temporal heterogeneity (Gonzalez and Holt 2002). We summarize the findings of experiments and models done to date on the inflationary effect. Third, we suggest that a clear understanding of the inflationary effect enriches our understanding of a critical dimension of population biology, with implications for species persistence and the spread of infectious disease. We argue that failing to grasp this effect hampered the management of the SARS-CoV-2 pandemic. We finish by identifying future directions in ecology, evolution, and conservation biology that involve spatiotemporal heterogeneity and the inflationary effect. Our emphasis is on conceptual issues and illustrative examples in order to make the mathematics more intuitive and accessible, but key references for deeper investigation are provided for interested readers.

Spatiotemporal Heterogeneity

Among the simplifying assumptions of classical metapopulation models, perhaps the most consequential is the assumption that extinction rates (and colonization rates) are independent across patches, which we argue here often implies the presence and influence of spatiotemporal heterogeneity. Spatiotemporal heterogeneity denotes how the spatial pattern of conditions changes over time. Spatiotemporal heterogeneity is a form of variability in the environment that is apparent only when one considers space and time together. Though the founders of metapopulation theory recognized this issue (e.g., Hanski 1998), an explicit discussion of this fundamental assumption is encountered infrequently in the literature and deserves special attention.

Spatiotemporal heterogeneity occurs when the spatial patterning of conditions affecting fitness (or growth rates) changes over time (equivalently, temporal patterning differs across space). It can be viewed as the variation remaining once accounting for average variation in space and time (fig. 1). A statistical decomposition of total variation in some defined space and time reveals three components: σ^2_S, the variance in the average spatial pattern across time; σ^2_T, the variance in the average temporal pattern across space; and σ^2_{ST}, spatiotemporal variability (box 1; for alternative but conceptually similar definitions, see Chesson 1985; Melbourne et al. 2007; Johnson and Hastings 2023; Schreiber 2025). Our focus is on σ^2_{ST}, which is a distinct form of variability from

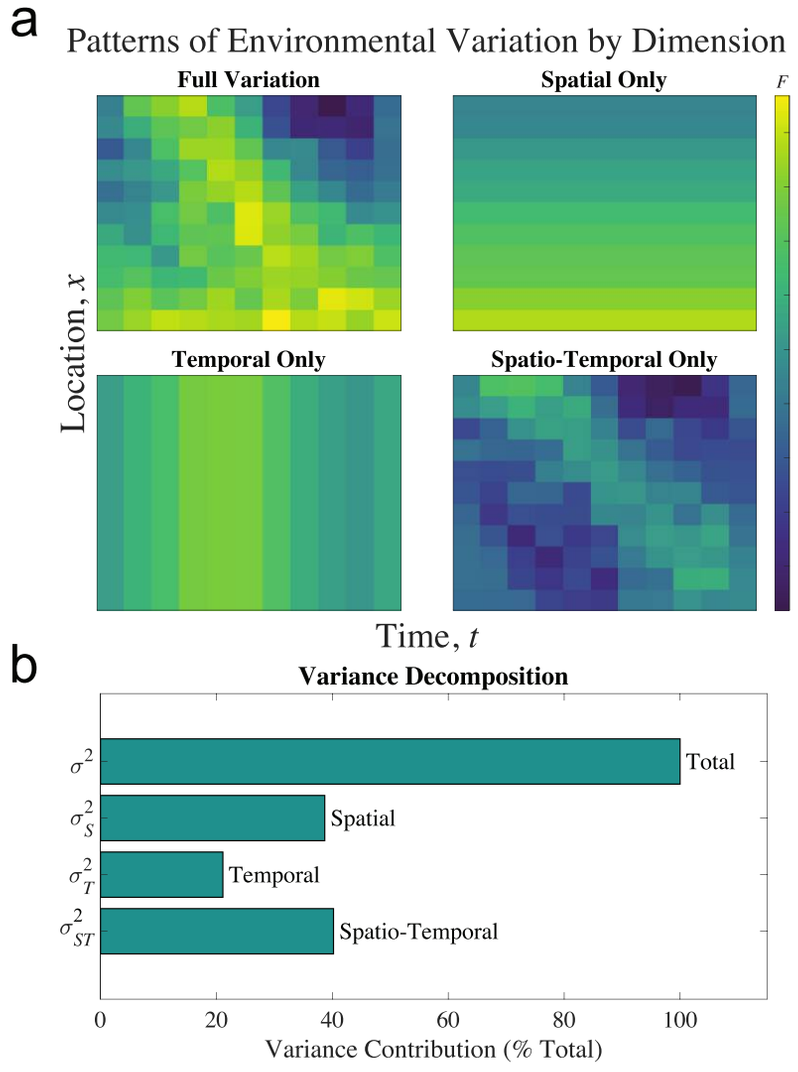

Figure 1: Hypothetical landscape with variability in conditions affecting fitness. *a*, Spatial locations are aligned vertically, and time points are aligned horizontally. Averaging values across time (i.e., horizontally) gives $\tilde{F}_x$, a perspective that illuminates differences in average conditions across locations. Averaging values across space (i.e., vertically) gives $\bar{F}_t$, a perspective that illuminates differences in average conditions over time. The remaining variation is spatiotemporal. Adding together the variation in the "spatial only," "temporal only," and "spatiotemporal only" panels recovers the "full variation" panel. *b*, Decomposition of total variation across space and time in fitness factor for landscape in *a*.

temporal and spatial variation. It can constitute from 0% of total variability (i.e., the spatial pattern is unchanging in time) up to 100% (i.e., average conditions in time are equal across locations, but conditions nonetheless vary like a shifting mosaic across locations and over time).

Spatiotemporal heterogeneity occurs in both abiotic and biotic dimensions of the environment. In both cases, the spatial pattern of the environment fluctuates over time. Temperature and precipitation are typical abiotic examples because, at any time, some places are hotter and wetter than others, but the places that are hottest and wettest change over time. Spatiotemporal heterogeneity can also arise from interactions between different abiotic factors varying across space and time. For example, in a landscape with many lakes and ponds differing in area and depth, larger and deeper water bodies are buffered from fluctuations in physical factors, such as temperature, compared with smaller and shallower water bodies. Thus, the water body with the highest (or lowest) temperature is likely to change over time. These abiotic mechanisms may impact a focal species directly or indirectly, for example, by directly affecting another species with which that focal species interacts.

Box 1: Mathematical description of spatiotemporal heterogeneity

To illustrate how to quantify spatiotemporal heterogeneity, consider a landscape with locations and time indexed by x and t, respectively. Let $F(x, t)$ measure some factor influencing the fitness or growth rate of individuals found in x at t.

A characterization of this factor that does not include temporal effects is a *spatial-only* perspective. A measure for the average condition over time in location x is $\tilde{F}_x = E_t[F(x,t)]$, where E_t is an average over time, indicated by a tilde. The spatial variation in $\tilde{F}_x$, $\sigma^2_S = \mathrm{Var}_x(\tilde{F}_x)$, measures *purely spatial variation* (Var_x is the variance over space).

A characterization of variation ignoring space is a *temporal-only* perspective. A measure for the average condition at time t across the entire landscape is $\bar{F}_t = E_x[F(x,t)]$, where E_x is an average across space and is indicated by an overbar. The temporal variation in $\bar{F}_t$, $\sigma^2_T = \mathrm{Var}_t(\bar{F}_t)$, gauges *purely temporal variation* (Var_t is variance over time).

Given these definitions of pure spatial and pure temporal variance, the total variance is

$$\mathrm{Var}(F) = \sigma^2_S + \sigma^2_T + \sigma^2_{ST},$$

where σ^2_{ST} measures *spatiotemporal variation*. The expression for spatiotemporal variation is (see supplementary material S1 for derivation)

$$\begin{aligned}\sigma^2_{ST} &= E_t[\mathrm{Var}_x F(x,t)] - \mathrm{Var}_x(E_t[F(x,t)]) \\ &= \text{time average of the variance across space} - \text{pure spatial variance.}\end{aligned}$$

The quantity σ^2_{ST} represents the amount of variation over time of the spatial distribution of conditions. An equivalent representation represents the amount of variation in space of the temporal pattern of conditions (for details, see sec. S1 of the supplemental PDF).

A special form of biotic spatiotemporal heterogeneity comes in the form of spatially asynchronous population and community dynamics (Shoemaker et al. 2022). Asynchronous population dynamics are a form of spatiotemporal heterogeneity because the temporal patterns of abundance differ across space. Asynchronous ecological dynamics can arise from spatially asynchronized physical environmental conditions (Reuman et al. 2023) but can also occur in homogeneous physical environments because of complex processes involving density dependence, dispersal, chance events, and interspecific interactions (Levin 1974; Keeling et al. 2000; Vasseur and Fox 2009; Gouhier et al. 2010). For example, slight differences in initial conditions, paired with chaotic dynamics, can generate large deviations in population trajectories among locations (Hassell et al. 1991; Holt 1993). Moreover, spatially asynchronous population sizes can occur in small populations heavily subject to demographic stochasticity, which may lead to chance extinctions in small, isolated populations (Gaggiotti and Hanski 2004).

While asynchrony and spatiotemporal heterogeneity are related, they are not the same. Asynchrony always implies spatiotemporal heterogeneity but is not necessary for spatiotemporal heterogeneity. Even perfectly synchronized dynamics in space can have a spatiotemporal component if the magnitude of fluctuations in time differ across locations (see sec. S1.1 of the supplemental PDF). For example, temperature in differently sized water bodies could exhibit perfectly synchronized fluctuations across locations but with different magnitudes. These fluctuations, while spatially synchronous, nonetheless characterize spatiotemporal heterogeneity.

Simple Models of Spatiotemporal Heterogeneity: Spatial Occupancy Models

Levins (1969) introduced the metapopulation concept to deal with the complexities generated by modeling spatiotemporal heterogeneity. While this is often overlooked in more contemporary descriptions, environmental heterogeneity was at the forefront of Levins's mind when developing the concept. His original article articulating the metapopulation model is titled "Some demographic and genetic consequences of environmental heterogeneity for biological control." He recognized that environmental conditions differing across space and time could cause populations to fluctuate wildly, oftentimes causing local extinctions. But sites do not remain empty because reproductively viable individuals from surviving populations can immigrate and recolonize recently extinct populations.

Localized extinctions and subsequent recolonizations are foundational in classical metapopulation models of occupancy.

Classical occupancy models build on the following canonical form:

$$\frac{dp}{dt} = cp(1 - p) - ep, \tag{1}$$

where p is the proportion of patches currently occupied, e is the rate at which populations go locally extinct, and cp is the rate at which unoccupied patches become occupied (c is the colonization rate per occupied patch). Model (1) describes landscapes with many patches, where each patch has the same extinction rates and where recolonization does not depend on the spatial position of empty patches (Hanski 1997, 1998). It predicts that if the extinction rate is lower than the colonization rate ($e < c$), the fraction of occupied patches grows logistically to $p^* = 1 - e/c$. Though local extinction is inevitable everywhere, recolonizations allow metapopulation persistence.

A crucial assumption of model (1) is that local extinctions are not synchronized; otherwise, recently extinct populations would have no sources for recolonization. Asynchrony in model (1) is implied from a technical feature of exponential rates. Model (1) with no recolonization (i.e., $c = 0$) leads to occupancy that declines at an exponential rate given by $dp/dt = -ep$. Exponential rates occur when individual events are independent of each another and independent over time and so are asynchronous. Such stochastic processes at the level of populations of individual events are described by Poisson distributions when measuring the number of events (here, extinctions) and exponential distributions when measuring the length of events across those populations (here, time to extinction). Others have pointed out the inherent assumption that extinctions are asynchronous (Chesson 1981; Hanski 1998; Hoopes et al. 2005), but this insight is rarely at the forefront of the discussion of metapopulations and can be overlooked (although see Chesson 1985; Harrison and Quinn 1989; Petchey et al. 1997).

To illustrate this subtle assumption and its consequences, we simulated a finite patch version of model (1) (fig. 2; for details, see sec. S2 of the supplemental PDF). In this model, spatiotemporal variability can be controlled with the joint probability of extinctions across patches over time. If we assume independence of extinction events across space and time, the model corresponds to a finite-patch version of equation (1) with strong spatiotemporal heterogeneity because the temporal patterns of extinction-causing factors differ among patches (fig. S2*c*; figs. S1–S6 are available online). If instead there are correlated extinction events across patches, temporal patterns of extinction are similar across patches, reducing spatiotemporal heterogeneity.

We tune the level of spatiotemporal heterogeneity with ρ_E, the correlation between any two patches in environmental conditions affecting extinction. The parameter ρ_E represents a latent variable that nonlinearly determines extinction (fig. S2). For example, a metapopulation of a focal species of plant might become locally extinct if herbivore abundance were above a particular threshold. In that case, ρ_E describes the correlation of herbivore abundance across patches. When $\rho_E = 0$, herbivore abundance is independent across patches and so extinction events are independent across patches, and all variation in extinction is spatiotemporal ($\sigma^2_{ST} > 0$; $\sigma^2_T = 0$). When $\rho_E = 1$, herbivore abundance is perfectly correlated across patches and so extinction in one patch implies extinction in all (i.e., no spatiotemporal variation;, $\sigma^2_{ST} = 0$), and all variation in extinction is temporal ($\sigma^2 = \sigma^2_T$). This model has no spatial heterogeneity in extinction ($\sigma^2_S = 0$) regardless of the value of ρ_E because all patches have the same average extinction probability.

Removing spatiotemporal heterogeneity in this model erodes metapopulation stability and persistence. With independent extinctions (i.e., $\rho_E = 0$), the population reaches a relatively stable patch occupancy (fig. 2, blue line), even in a finite patch model with a modest number of patches ($n = 50$). But when we break the assumption of independent extinction events across locations, the metapopulation is much less stable (fig. 2, green line). Occupancy fluctuates wildly because local extinctions, when they occur, typically occur over a large spatial domain, with many local populations impacted simultaneously. Even highly occupied metapopulations are vulnerable to drastic drops in occupancy because of highly synchronized extinction events, a finding that has been illustrated experimentally (Fox et al. 2017).

The large fluctuations caused by eroding spatiotemporal heterogeneity greatly increase the likelihood of metapopulation extinction. For example, a metapopulation of $n = 25$ patches with independent extinction events (i.e., strong spatiotemporal heterogeneity) persists an average of ~300,000 units of time (fig. 3*a*, dark purple points). Removing spatiotemporal heterogeneity by correlating patch extinction events reduces persistence times by several orders of magnitude (fig. 3*a*), despite little change in average occupancy (fig. 3*b*). This simple model shows (as do others; e.g., Fox et al. 2017) that the well-known stability of metapopulation models results from an implicit assumption of strong, persistent spatiotemporal heterogeneity.

Metacommunities: Spatiotemporal Heterogeneity in Species Interactions

A natural extension of metapopulation models is to consider multiple interacting species. Patches now represent local arenas harboring communities, connected by dispersal,

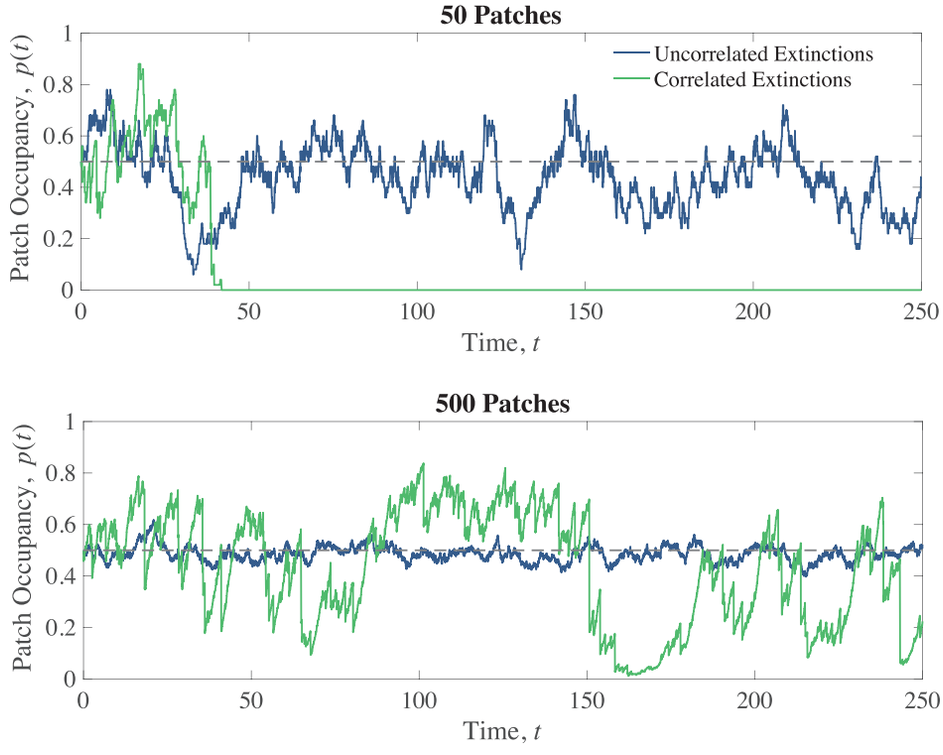

Figure 2: Finite patch version of Levins's metapopulation model under different degrees of asynchrony of local extinctions and for low and high patch numbers. Blue lines show dynamics under the conventional assumption that environments influencing local extinction are uncorrelated across patches, that is, are spatially asynchronous ($\rho_E = 0$). Green lines show dynamics under spatially correlated extinctions ($\rho_E = 0.75$). Simulation details can be found in the supplemental PDF. For all dynamics, $e = 0.25$ and $c = 0.5$ such that the infinite patch model predicts equilibrium occupancy of $p^* = 1 - e/c = 0.5$ (dashed lines).

the collection of which is a metacommunity (a term first used by Wilson 1992). Species' colonization and extinction rates in metacommunities reflect some combination of the physical environment, interspecies interactions, and demography. Metacommunity models can come in occupancy form (see, e.g., Hastings 1980) as well as patch form (e.g., Holt and Chesson 2016). Spatiotemporal heterogeneity in patch models—a rich and growing area of community ecology (Driscoll and Lindenmayer 2009; Leibold and Chase 2018; Lu 2021; Leibold et al. 2022)—is considered below. Here we show how a simple occupancy-based metacommunity formed by locally unstable interactions is stabilized by spatiotemporal heterogeneity.

Consider a specialist predator interacting with its prey. A specialist predator-prey metacommunity model is

$$\begin{aligned} \frac{dp}{dt} &= c_p p(1-p) - (e_p + c_p q)p, \\ \frac{dq}{dt} &= c_q qp - e_q q, \end{aligned} \tag{2}$$

where p is the fraction of habitat patches occupied by prey alone, q is the fraction occupied by both predators and prey, c_i is the colonization rate of patches of type i ($i = p, q$), and e_i is the extinction rate of patches of type i (e.g., the prey alone or the prey together with the predator).

Models such as (2) share assumptions with Levins's metapopulation model except that now extinction and colonization rates depend on other species. Patches occupied by prey alone change state independently of the predator (e.g., because of disturbance) with an extinction rate of e_p. They are colonized by the predator at a rate proportional to the availability of prey-only patches and predator prevalence ($c_q pq$). The predator greatly limits prey numbers in co-occupied patches, and as such, patches occupied by the predator do not provide prey colonists to empty patches. Model (2) assumes that predators become locally extinct only when their prey in a patch become extinct and do not persist once their prey are gone. More elaborate models relaxing these assumptions about extinction (Holt 1997) and assuming different influences of predators on prey colonization lead to comparable effects, albeit with some different twists (Holt 1997; Poethke et al. 2010).

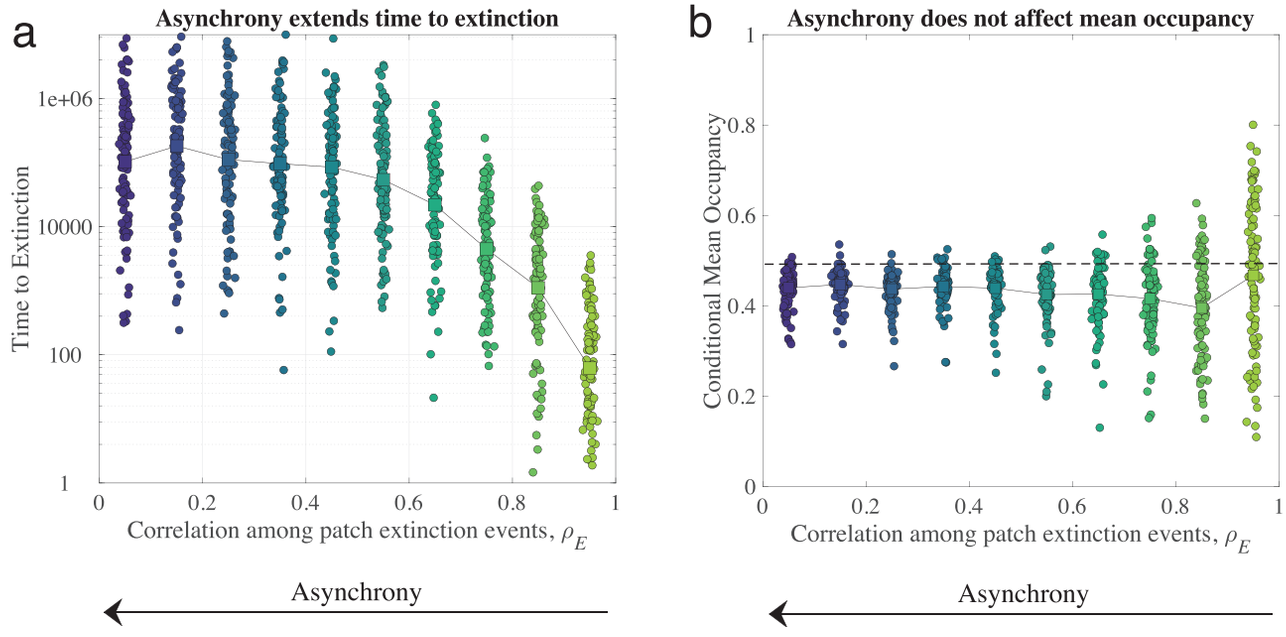

Figure 3: Effect of spatially correlated extinction events on metapopulation stability. *a*, Metapopulation extinction times for replicate simulations. *b*, Corresponding conditional mean occupancy. Squares connected by lines are the geometric mean extinction times (*a*) and mean conditional mean occupancy (*b*) over all replicate simulations. The parameter ρ_E refers to the correlation coefficient for all pairwise latent variables describing environmental variables determining extinction in patches (details in sec. S2 of the supplemental PDF). All simulations had 25 patches, 13 of which were initially occupied, with $e = 0.5$. There are 100 replicate simulations for each ρ_E value. Dashed line in *b* is the equilibrium occupancy in the original Levin's model. Mean occupancy in the stochastic model is lower than in the deterministic model, which we attribute to a combination of below-average occupancy just prior to extinction and because equilibrium occupancy is a nonlinear concave function of the average colonization rate within a single simulation (which here varies slightly between simulations). This stochasticity in colonization in metapopulation models depresses average occupancy by Jensen's inequality (see box 1 of Peniston et al. [2024] for arguments to this effect).

Metacommunity models such as (2) often exhibit stability despite locally unstable interactions between species within patches (Levin 1974; Gravel et al. 2016). Large-amplitude predator-prey fluctuations arise in spatially and temporally homogeneous local environments with well-mixed species (May 1972). Such interactions are difficult to sustain experimentally (though see Blasius et al. [2020] for a laboratory success) yet are generally stable in a metacommunity framework (Hastings 1977; Gouhier et al. 2010; Pillai et al. 2011). This regional stability reflects spatiotemporal heterogeneity, which arises because local extinctions (either in predators or prey) occur independently across locations, as in metapopulation model (1), and colonizations likewise are independent. Independent predator-induced prey extinctions imply that predators are unevenly distributed across space and that the spatial pattern of occupancy constantly shifts over time, a diagnostic feature of spatiotemporal heterogeneity. Synchronous predator colonization or prey extinction events generate large-scale oscillations comparable to those of figure 2, with a high likelihood of regional extinction in realistic models, a prediction empirically validated in the lab (Fox et al. 2017).

Digging Deeper: Simple Source-Sink Systems with Spatiotemporal Heterogeneity

The stabilizing effects of spatiotemporal heterogeneity can be difficult to recognize in metapopulation models of occupancy, and the exact interplay between environmental heterogeneity, dispersal, and population growth can be difficult to discern. However, this interplay is revealed in patch models where the factors affecting local demography and movement are explicit. We review one line of inquiry that uncovers a key emergent effect of spatiotemporal variation in patch models with explicit local demography and movement.

An early illuminating example of the effects of spatiotemporal heterogeneity was illustrated by Gonzalez and Holt (2002), who considered a single sink patch supported by constant immigration from a source patch. Sink populations

(i.e., local populations that become extinct in the absence of any immigration) may persist given constant immigration from a source population, which is a population that can persist indefinitely in the absence of movement (Van Horne 1983; Holt 1985; Pulliam 1988; Runge et al. 2006). Gonzalez and Holt (2002) envisioned a sink that was only so on average over time. Transient phases of locally favorable conditions might allow a population to temporarily grow without immigration (and so the population may fluctuate and temporarily increase), but eventually, without recurrent immigration, given its sink status, it declines, and the population becomes locally extinct. This spatial scenario is a very simple form of spatiotemporal heterogeneity because a constant source of immigration implies constant conditions in the source, unlike those in the sink. Our measure of spatiotemporal variance applied to Gonzalez and Holt's (2002) model shows that $\sigma^2_{ST} = \sigma^2_r/4$, where σ^2_r is the variance in sink growth rates (for more details, see sec. S3 of the supplemental PDF).

The spatiotemporal heterogeneity introduced by variation in the sink inflates time-averaged population sizes in the sink (sometimes by orders of magnitude; fig. 4). Gonzalez and Holt (2002) termed this phenomenon the inflationary effect, and we refer to it as an inflationary effect of the environment on abundance, in which the joint presence of spatiotemporal heterogeneity and dispersal increases average total population abundance across the metapopulation. This effect was rigorously tested and demonstrated empirically in a microcosm experiment with source-sink populations of the protozoan *Paramecium tetraurelia*, buffeted by temporally varying thermal conditions (reported in Gonzalez and Holt 2002). It occurs because runs of good conditions for growth cause large upswings in population size that are greater than declines in population sizes during poor times for growth. The rate of population decline during poor times is buffered by recurrent immigration from the source (preventing local extinction). Thus, the effects of favorable conditions over time outweigh the effects of unfavorable conditions, even if good and poor times are equally frequent.

Somewhat remarkably, the inflationary effect has also been shown theoretically to promote the persistence of species in landscapes composed entirely of sink patches (Roy et al. 2005). In other words, in every location on the landscape, a local population isolated from immigration cannot persist, but nonetheless the ensemble persists when patches are linked by moderate dispersal. This point is worth reiterating. In such landscapes, there is no persistent source habitat anywhere in the landscape, but dispersal (not too much; see sec. S4.1 of the supplemental PDF) to neighboring locations can suffice to allow all populations to persist. This boost in regional population size promotes

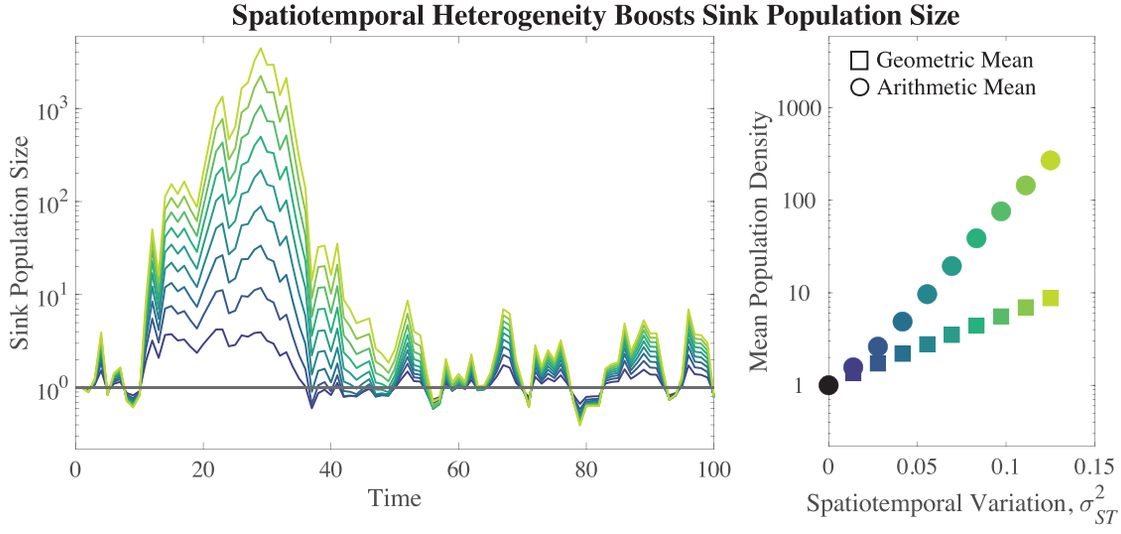

Figure 4: Sink population dynamics with fluctuating growth rate and constant immigration from source population. Sink dynamics follow $N(t+1) = N(t)e^{r(t)} + I$, where $r(t)$ is the per capita growth rate without immigration and I is the density of immigrants each time step. Here $r(t)$ is normally distributed and independent over time, with mean $\bar{r} = -0.2$ and standard deviation σ_r. Lines represent 10 equally spaced values of σ_r between $\sigma_r = 0$ (black line) and $\sigma_r = 0.5$ (yellow line). When σ_r is larger, the environment is more variable in the sink (i.e., good times are more favorable to growth and poor times are more unfavorable to growth) without changes in the average suitability of the environment. Right panel shows the corresponding geometric and arithmetic mean abundances in the sink as a function of the calculated spatiotemporal variation in the model ($\sigma^2_{ST} = \sigma^2_r/4$). We set $I = 1 - e^{-0.2} \approx 0.18$, which simply makes the equilibrium density of the sink 1 in a constant environment. All cases start with the same initial conditions and have the same environmental sequence. Further details are in section S3 of the supplemental PDF.

persistence and critically depends on spatiotemporal variation in growing conditions among patches. It is a specific case of paradoxical persistence of mixed dynamics systems with strong heterogeneity (see the excellent review of such systems in Williams and Hastings 2011).

A microcosm study (Matthews and Gonzalez 2007) prompted by this theoretical result convincingly demonstrated that spatiotemporal heterogeneity permits metapopulation persistence. Matthews and Gonzalez set up a microcosm of two local populations of *Paramecium aurelia* under fluctuating temperatures. In isolation, both became extinct (i.e., were sinks). When coupled by dispersal, extinction occurred in both patches for treatments with synchronous temperature fluctuations across patches, but both populations persisted in treatments with asynchronous temperature fluctuations across the two patches. They further showed that positive temporal autocorrelation boosted the inflationary effect on sink population sizes, because runs of favorable conditions allowed the boost in population sizes to be greater. A comparable result was found for host-parasite dynamics in metapopulations of *Paramecium caudatum* and its bacterial parasite *Holospora undulata* (Duncan et al. 2013). The key finding of that study was that temporally autocorrelated and spatially asynchronous variation in temperature (i.e., spatiotemporal heterogeneity) allowed infected host populations to maintain sizes equivalent to uninfected populations, despite negative demographic impacts of parasites on infected individuals.

These studies demonstrate a very general pattern: spatiotemporal heterogeneity in growth rates can robustly allow for persistence of species and increase their abundance in metapopulations linked by moderate dispersal. On the one hand, these experiments and models are remarkable in demonstrating how populations of sinks can persist when coupled together. On the other hand, these results are analogous to the classical stability results of metapopulations because metapopulations persist despite no individual patch persisting on its own without the others. One might apply to metapopulations as a motto the famous quip ascribed to Benjamin Franklin, "We must all hang together, or assuredly we shall all hang separately."

What Is the Inflationary Effect and How Does It Work?

Models show that spatiotemporal heterogeneity can inflate time-averaged per capita growth rates (Schreiber 2010) and abundance (Roy et al. 2005) and help to reveal the requirements for inflation to occur. Put simply, the inflationary effect is the result of spatiotemporal heterogeneity inflating some aspect of population growth at the scale of the metapopulation, such that it exceeds growth under some simple average of local conditions. The requirements for inflation in patch models are (1) temporal variation in patch growth rates, (2) a less than perfect spatial correlation in those growth rates (i.e., spatial correlation below 1), (3) some movement among patches, and (4) temporal autocorrelation in growth rates. The combination of temporal variation and low spatial correlation in growth rates constitutes spatiotemporal heterogeneity. The combination of movement and temporal autocorrelation allows individuals sufficient time to build up in temporarily favorable locations and disperse across space. As local populations grow, more individuals emigrate, even if the locations into which they immigrate are currently poor for growth. Given spatiotemporal heterogeneity, favorable conditions in one patch imply that emigrants from there are likely to immigrate to a temporary sink, boosting numbers there. Temporary sinks disproportionately benefit from immigration because the influx maintains minimum population sizes. Populations with slightly larger sizes grow faster (in absolute, not per capita terms) when the environment eventually turns, as illustrated in the sink model with constant immigration above (fig. 4; for model details, see sec. S3 of the supplemental PDF). Without temporal autocorrelations, environments shift before populations can build up substantially in transiently favorable locations.

To make this qualitative description of inflation more precise, consider the following mathematical description of the inflationary effect on growth rates. Mathematical descriptions are available for discrete time (Schreiber 2010, 2025; Johnson and Hastings 2023), but we present one for continuous time where the math is (slightly) less painful and helps hone one's intuition. Consider a patch model with n connected patches, where $N_i(t)$ is the local density in a patch i at time t, $r_i(t)$ is the (possibly density-dependent) local per capita growth rate, m_{ij} is the per capita movement rate from patch i to j, and $m_i = \sum_j m_{ij}$ is the (possibly density-dependent) total emigration rate from patch i. The dynamics in patch i follow

$$\frac{dN_i}{dt} = \underbrace{r_i(t)N_i}_{\text{local growth}} - \underbrace{m_i N_i}_{\text{emigration}} + \underbrace{\sum_{j\neq i} m_{ji}N_j}_{\text{immigration}}, \tag{3}$$

which allows for time- and location-dependent growth rates. (We assume for simplicity no mortality during dispersal.)

The inflationary effect in model (3) can be measured in terms of the linear relationship between local growth rates, $r_i(t)$, and local relative density, $\nu_i(t) = N_i(t)/\bar{N}(t)$ (where $\bar{N}(t)$ is the average density across the n patches). It can be written as (derivation in sec. S4 of the supplemental PDF)

$$\text{inflationary effect} = E_t[\text{cov}_i(r_i(t), \nu_i(t))] - \text{cov}_i(\tilde{r}_i, \tilde{\nu}_i). \tag{4}$$

The inflationary effect is measured as a comparison of covariances between local density and local growth rates in different contexts. The first covariance in equation (4) is measured from the full model given by equation (3) with spatiotemporal heterogeneity. The second covariance is measured in a reference environment where spatiotemporal heterogeneity has been removed by assuming that growth rates are fixed at their average across time. This comparison thus isolates the effect of spatiotemporal heterogeneity (for more discussion, see sec. S4 of the supplemental PDF; for an example of the calculation with the disease model used below, see fig. S6).

Equation (4) fundamentally measures how species' dispersal patterns interact with the spatiotemporal structure of the environment to alter regional population dynamics. The determining factor for inflation is whether the distribution of individuals in the metapopulation on average matches the distribution of local growth rates. As such, it measures the ability of populations to track good locations that constantly shift in time and space. Expression (4) may be positive, negative, or zero, reflecting the relative ability of individuals to reach favorable conditions, whether passively or actively. When positive, individuals in the metapopulation are, on average, concentrated in better than average spatial locations. When negative, individuals in the metapopulation are, on average, concentrated in poorer than average spatial locations. When zero, population density is, on average, random with respect to local patch growth rates. (Deriving explicit expressions for this quantity is analytically challenging; however, some approximations are possible [see Schreiber 2025].)

The sign of the inflationary effect depends in large part on the details of dispersal and its relation to factors affecting fitness in the metapopulation. Prior studies studying the inflationary effect have almost always assumed constant, identical, and symmetrical rates of dispersal between all patches (i.e., fitness-independent dispersal). In such cases, the inflationary effect is positive, provided that dispersal rates are not too high (exactly how much is too high depends on the magnitude and temporal autocorrelation structure of growth rates; for more details, see sec. S4 of the supplemental PDF). Fitness-dependent dispersal—which has not been rigorously studied in terms of the inflationary effect—should strengthen inflationary effects, as it has been shown to enhance persistence in some systems (Poethke et al. 2010). For instance, if organisms show some breeding site fidelity in good years and local environments are positively autocorrelated in fitness over time, this behavioral tendency helps populations persist in spatiotemporally varying environments (Schmidt 2004).

We suspect that organisms with environmentally forced dispersal—such as happens with wind-dispersed plant propagules and aquatic and marine organisms dispersing with water currents—may experience limited (or no) benefits of the inflationary effect. In some cases, the pattern of environmentally determined dispersal could lead individuals away from temporarily high fitness locations, creating negative inflationary effects. For example, Keddy's (1982) study on the sea rocket (*Cakile edentula*) in Nova Scotia dunes demonstrated a strong source-sink dynamic. Populations near the sea are productive yet rare because wind from the sea strips seeds there, depositing them in the dune interior. Populations are abundant inside the dunes, even though they are sinks (local births $<$ local deaths, across all measured densities). Such directional dispersal out of sources into sinks produces negative average covariance between local abundance and local fitness (deflationary effects).

While there has been a great deal of work on the inflationary effect in a variety of models, there is still much that is unknown. Studies have shown that the effect exists robustly in models with explicit resource dynamics, density dependence, demographic stochasticity, and competition between species (although the magnitude of the effect may differ across contexts; Holt et al. 2003) and occurs over a broad range of parameter space in both discrete- and continuous-time models (Schreiber 2010; Katriel 2022; Benaïm et al. 2023). Among the important unknowns is the relationship between inflationary effects on abundance and on growth. Inflated abundance in many cases implies inflated population growth when rare at the metapopulation scale, as is illustrated by the case of persistence in a landscape of temporally varying, on-average sinks. However, it is unclear whether inflated growth when rare always leads to inflated abundance at a long-term equilibrium. We suspect that the answer lies in how density dependence acts on the landscape to influence how variation in fitness factors translates into long-term average abundance. Negative inflationary effects are theoretically possible but to our knowledge have never been demonstrated empirically. Another critical unknown is what role life history plays in modulating the inflationary effect and the impact of dispersal costs, as most prior modeling studies assume unstructured populations and complete survival during dispersal. Future modeling work should fill these gaps.

Although the theory has been satisfactorily demonstrated in several laboratory experiments with model species, our understanding of the inflationary effect in natural systems is limited. But the inflationary effect seems most likely for species living in environments with the characteristics outlined in table 1, which could provide useful indicators for choosing apt systems to empirically study it. The inflationary effect remains a niche concept in population and community ecology, despite its apparent connection to the basic concepts of persistence in metapopulation and metacommunity theories. We hope that this review—and the

Table 1: Features necessary for inflationary effect in natural systems

Empirical pattern	Link to inflationary effect measure (eq. [4])
Spatiotemporal variation in fitness-affecting factor	Variation in local growth rates across space and time, $r_x(t)$
Spatial distributions of individuals that are nonrandom with respect to fitness factor	Spatial variation in relative density, ν_x, and positive cov(r_x, ν_x)
Temporal changes in nonrandom distribution of individuals over space	Variation in local density across space and time, $\nu_x(t)$
Undirected passive dispersal or environmental tracking	Possibility that population is concentrated in locations and times of higher than average growth (positive cov($r_x(t)$, $\nu_x(t)$), on average)

case studies from epidemiology provided below—spark interest in the concept, especially among empiricists.

Spatiotemporal Heterogeneity and Infectious Disease: A Case Study of COVID-19

Our emphasis thus far has been conceptual, with illustrative examples from microcosm experiments with protozoans and free-living dune plants, but the inflationary effect may be particularly common in host-parasite (Duncan et al. 2013) systems for two reasons. First, individual hosts even within the same host species can vary substantially in their immunity, behavior, and physiology in ways that can generate spatiotemporal heterogeneity within and among host populations. Second, pathogen dynamics are often fast in terms of absolute pathogen numbers and host infections. Quickly growing pathogens in currently favorable local host populations can spread to new ones and can do so quickly when conditions change.

The inflationary effect of pathogen growth may be present at multiple scales in infectious disease systems but can be categorized schematically into either the within-host scale or the among-host scale. Linking within-host dynamics to among-host dynamics is a challenge, with many avenues yet to be explored (e.g., analogs of emigration coupled to transmission altering within-host pathogen dynamics; see Barfield et al. 2015). This is an important theme, but here we focus on only the among-host scale, considering populations of individual hosts and metapopulations of hosts (see e.g., Cliff et al. 2000).

Host populations can be described at both local and regional scales. Local host populations are metapopulations from the perspective of pathogens and parasites harbored within those individual hosts. Within a local host population, transmission of infectious pathogens to uninfected hosts is in effect colonization of empty patches, and pathogen clearance (or host death) is a form of local extinction for the pathogen. Susceptible-infectious-recovered (SIR) models in epidemiology are metapopulation models where one simply tracks pathogen occupancy (are individual hosts infected or not?) rather than pathogen load. In SIR models, local persistence of a pathogen relies on stabilizing effects of spatially uncorrelated infections and clearance, analogous to colonizations and extinctions, respectively, in metapopulation occupancy models. Metapopulations at the host scale involve local host populations coupled by host movement (or possibly vector movement). For the pathogen, these regional ensembles are "meta-metapopulations" and can be represented as multisite SIR models that include movement among local arenas of infection.

Spatiotemporal heterogeneity of host-pathogen interactions can arise in many ways related to individual host condition (e.g., physiology and immunity) and local conditions (e.g., host abundance), but behavior—which differs both within and between populations—is often key to infectious disease transmission and creates potent spatiotemporal variation at different spatial scales. We will focus as an example on infectious disease dynamics within our own species. Broad, geographically distinct populations of human hosts behave differently owing to different local public health policies, demography, economics, and social norms. Local and regional drivers can interact to contribute to spatiotemporal heterogeneity, such as when bottom-up changes in individual behavior magnify or dampen top-down forces, such as imposed public health measures (e.g., differences among locations in social expectations about the importance of nonpharmaceutical control measures can modulate their impact).

In 2020, early during the COVID-19 pandemic, many of the present authors noticed the potential for broadscale spatiotemporal heterogeneity and asynchrony in disease transmission to influence the spread of SARS-CoV-2, the causal agent of COVID-19. Initially, there were few options to combat SARS-CoV-2. In the absence of therapeutics and vaccination, the main approaches to slow and limit its spread—thereby reducing stress on health care infrastructure—were nonpharmaceutical interventions (e.g., masking, social distancing, closing of nonessential business places, lockdowns; hereafter, interventions) that modified host behaviors. The timing, nature, and efficacy of interventions varied across time and space as social, economic, and epidemiological conditions changed, and this shifting

mosaic of control efforts could have caused substantial spatiotemporal heterogeneity in the transmission rate of the pathogen.

To illustrate this idea, consider a version of the model used by Kortessis et al. (2020) to explore potential consequences of spatially asynchronous interventions on the pandemic (details in sec. S5 of the supplemental PDF). The model simplifies the world to two patches (e.g., cities or other discrete political entities) of human hosts linked by movement, including movement of asymptomatic infected individuals. Disease dynamics within each patch are described by an SIR model (with well-mixed hosts within each patch), and all epidemiological parameters are identical between patches except for $\beta(x, t)$, the transmission rate in location x at time t. For simplicity, we assume that $\beta(x, t)$ fluctuates between two values over time: β_0, a baseline transmission rate, and $\beta_0(1 - \epsilon)$, a transmission rate decreased by interventions with effectiveness ϵ. Each transmission rate lasts for a time T before switching (i.e., square wave temporal variation; fig. S3). The model includes the possibility for differences in the timing of interventions, controlled by a parameter Ω, which we refer to as the intervention overlap; Ω is the proportion of time the two patches have the same transmission rate. Intervention overlap controls the magnitude of spatiotemporal heterogeneity in this model because spatiotemporal variance is $\sigma^2_{ST} = (1 - \Omega)(\beta_0\epsilon/2)^2$ and, on a scale proportional to the total variation, is $\sigma^2_{ST}/\sigma^2 = (1 - \Omega)$ (see sec. S5 of the supplemental PDF). Hence, spatially synchronized policies ($\Omega = 1$) do not generate spatiotemporal variability, whereas spatially asynchronous policies ($\Omega < 1$) do.

The key finding is that spatially asynchronous interventions—when paired with some host movement between patches—inflate the metapopulation scale growth rate of infected hosts (fig. 5*a*). This is an instantiation of the inflationary effect for infectious diseases, where aspects of human behavior create spatiotemporal heterogeneity in the fitness of a respiratory virus. For any nonzero movement rate, the rate of pathogen spread at the metapopulation scale increases with spatial intervention asynchrony (i.e., smaller intervention overlap; fig. 5*a*). The effect is larger for more effective interventions (i.e., larger ϵ, generating greater variation in transmission over time; fig. S4) and when the duration of application of interventions is longer (larger T; fig. S5). Naturally, more intense interventions, when they occur, lower the growth rate of infectious hosts. However, given a specific intensity of interventions, spatially asynchronous interventions nonetheless inflate the rate of growth compared with equivalently intense interventions that are synchronized. Hence, when interventions are asynchronous, they must locally be more effective to achieve the same global effect as synchronized interventions.

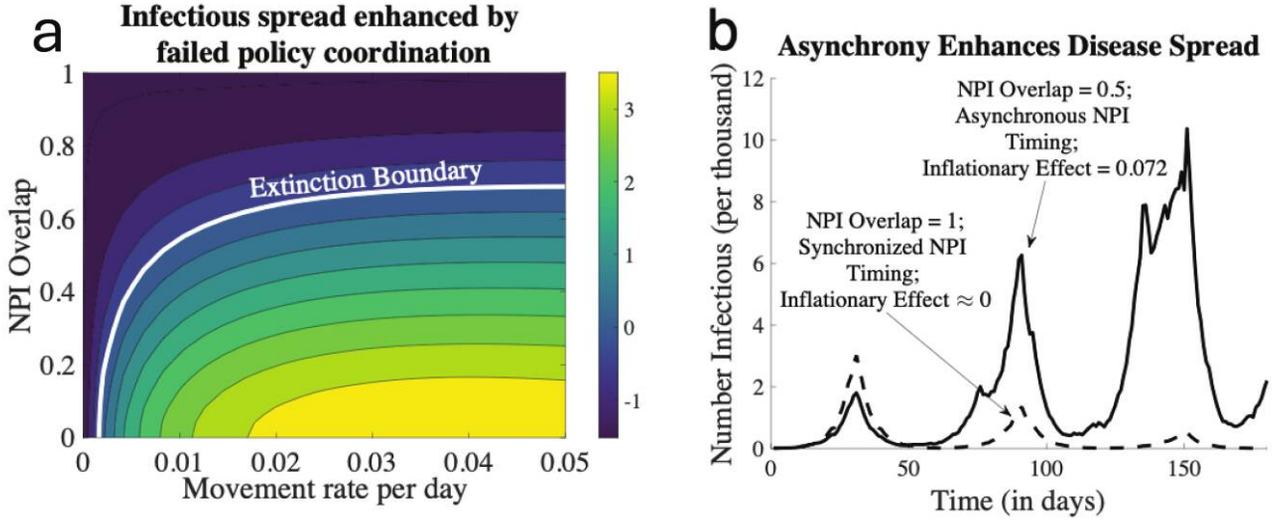

Figure 5: Inflationary effect in two-patch susceptible-infectious-recovered model. *a*, Metapopulation-scale growth rate and how it depends on overlap in application of nonpharmaceutical interventions (NPIs) and host dispersal. When interventions overlap less, they are less synchronized across space, and metapopulation-scale growth rates are higher (given fixed movement rates). *b*, Example dynamics from stochastic version of model. Parameters: infectious duration, 4.5 days; baseline transmission rate, $\beta_0 = 0.375$ day^{-1} (hence $R_0 \approx 1.7$); duration of intervention, $T = 30$; effectiveness of intervention, $\epsilon = 0.95$. In *b*, the movement rate is $m = 0.025$ day^{-1}. The inflationary effect is calculated using equation (4). Further details are in section S5 of the supplemental PDF.

These results extend to stochastic versions of the model, which show increasingly larger waves of infection when interventions overlap little in time compared with when they overlap completely (fig. 5*b*).

There is reason to believe that this phenomenon, while illustrated here with a very simple model, squarely pertains to the much more complex COVID-19 pandemic. Epidemiological data and evidence from cell phone data show that human mobility patterns during state-enforced interventions in the European Union in 2020 were sufficient to promote the inflationary effect in the presence of repeated statewide—but uncoordinated—lockdowns. Ruktanonchai et al. (2020) illustrated that if different countries in the European Union came out of lockdown at different times (thereby generating spatiotemporal heterogeneity, as was the case), then there would be many more infections and hospitalizations from COVID-19 than if countries and locations had come out of lockdown in a coordinated manner. Other authors have since modeled the timing of interventions in light of this phenomenon and found it to be quite general (Eksin et al. 2021; Zhang et al. 2021; Wang and Wu 2022; Berestycki et al. 2023). A general conclusion from this body of work is that optimal local public health strategies depend on decisions made by nearby localities (and the level of movement of hosts carrying the pathogen). In other words, spatiotemporal heterogeneity in disease transmission coupled with movement among locations could have substantively degraded the effectiveness of interventions during the pandemic.

The inflationary effect has likely played a role in the persistence of other human pathogens, such as measles. Prior to vaccination in the late 1960s, measles had synchronized biennial epidemics across England and Wales. Bolker and Grenfell (1996) documented how widespread vaccination eliminated large epidemics, which along with movement had been the putative causative synchronizing factor across locations. In effect, vaccination weakened local transmission sufficiently that measles dynamics were decoupled across space. Spatial asynchrony following vaccination was thus hypothesized to reduce the chance of regional extinction of measles. Unfortunately, in line with this prediction, measles in the United Kingdom is far from being eliminated, and eradication targets are still being chased (Winter et al. 2022) decades after the introduction of a highly effective vaccine. We conjecture that comparable effects are present—and often important for human health—in other infectious disease systems.

Other Applications of the Inflationary Effect in Ecology and Evolution

The inflationary effect has applications throughout ecology and evolution because it is about fundamental aspects of population growth: environmental heterogeneity coupled with dispersal. In hopes of stimulating study of the phenomena in new domains, we list some brief examples.

Conservation and Management

We argue that drivers of the inflationary effect can be leveraged to inform conservation and management decisions. The greatest threats to biodiversity—global change, habitat destruction, and overexploitation, among others (Brook et al. 2008; Bellard et al. 2022)—will modify the structure of the environment in ways that could either disrupt or foster the inflationary effect. Typically, more frequent extreme events (e.g., droughts and heat waves) synchronize populations (a generalized Moran effect; Hansen et al. 2020; see also Reuman et al. 2023), thereby weakening the inflationary effect. However, some evidence suggests that at sufficiently large scales, climate interactions with local heterogeneity decouple local spatial synchrony (Hansen et al. 2019). Similar ideas can be applied to management of fire-obligate communities, the complexity of which requires a carefully planned decision-making framework (Kelly et al. 2015). Managing burning regimes might be made more effective by thinking about the heterogeneity maintained or lost by the extent, timing, intensity, and spatial arrangement of managed fires (Noss 2018).

Scientists already recognize the importance of incorporating metapopulation processes for pursuing conservation priorities (Akçakaya et al. 2007), but considering the inflationary effect helps clarify the factors that promote persistence and stability of metapopulations. A common practice in conservation biology is to facilitate movement between local populations (e.g., with corridors) under the presumption that this enhances the benefits of the inflationary effect. While we agree that this is likely beneficial in many circumstances, the arguments here suggest that too much movement may move individuals away from temporarily favorable locations or degrade spatially asynchronous dynamics. Similar concepts apply in fisheries. Prescriptions about quotas might include considerations for how they promote or degrade spatial asynchrony at regional scales. Intense fishing on a few populations with temporarily high numbers can synchronize population dynamics across large scales, reducing the so-called population portfolio effect (Stier et al. 2020) and eroding stability provided by the inflationary effect.

Species Interactions

Natural enemy interactions have long been thought to be maintained by asynchronous dynamics. Effective predators risk overeating their prey and then suffering local extinction themselves. The spreading of risk among different

populations, loosely coupled by dispersal, is a likely reason for the persistence of many strong natural enemy interactions. In the classic experiments of Huffaker (1958), persistence of a predatory mite (*Typhlodromus occidentalis*) with a prey mite (*Eotetranychus sexmaculatus*) in a mesocosm comprised of an array of oranges depended on limited dispersal and the fact that local dynamics were asynchronous across space. This experiment inspired a later experiment with a bruchid beetle (*Callosobruchus chinensis*) feeding on beans and attacked by a pteromalid parasitoid (*Anisopteromalus calandrae*; Hassell and May 1988). Without spatial structure, the parasitoid rapidly overexploited its host and then became extinct (allowing the host to rebound). Host-parasitoid coexistence occurred only when each beetle was put in its own patch, with restricted dispersal among patches. Here, the physical environment was homogeneous (by experimental design), and spatiotemporal variation in each species' fitness arose entirely from within-species and between-species localized interactions.

The inflationary effect may also influence competitive interactions and species coexistence. One example is the competition-colonization trade-off. Classic models (e.g., Tilman 1994) that show persistence of rapidly colonizing but subordinate competitors require that patches be colonized asynchronously. The dynamics of the competitive dominant species—which in classic occupancy models immediately excludes competitive inferior ones—in effect generates a positively autocorrelated temporal environment for the local fitness of the inferior species. This can promote coexistence, provided there is asynchrony among patches in extinction and subsequent recolonization (Roy et al. 2005). Long et al. (2007) showed experimentally in a laboratory microcosm using bacterivorous protists that if the inferior (but not superior) competitor immigrates, temporal variation in growth rate boosts the time-averaged numbers of the inferior species, and this could even lead to the local extirpation of the locally superior (on average) species.

The inflationary effect also underpins the spatial insurance hypothesis (Loreau et al. 2003; Shanafelt et al. 2015; Thompson et al. 2017), which posits that biodiversity provides stability to ecosystem functioning across a metacommunity. According to this hypothesis, stability stems from the interaction between dispersal, differences among competing species in their use of the environment, and spatiotemporal environmental fluctuations. If different local communities experience distinct temporal patterns of environmental conditions, species in a local community well adapted to their local environment will thrive and supply emigrants (as a temporary source) for a finite period before the environmental state of the patch switches. Dispersal ensures that species adapted to the new environmental conditions locally are available as immigrants to replace less adapted species as the local environment changes. As a result, biodiversity enhances and buffers ecosystem processes by virtue of complementary inflationary growth among species in the metacommunity. Factors that synchronize population dynamics across ecosystems (Reuman et al. 2023) or constrain dispersal will erode the multispecies inflationary dynamics that stabilize metacommunities and thus their ecosystem functions.

Genetic Variation and Evolutionary Dynamics

Our focus has been on ecological consequences of spatiotemporal variation and the inflationary effect, but there are doubtless evolutionary effects, although they are much less explored. Wieczynski and Vasseur (2016) demonstrated that the inflationary effect could promote the maintenance of intraspecific genetic variation when different genotypes are differentially superior at distinct times, and they showed that overall population sizes could thereby increase and promote population persistence (the genetic analog to Loreau et al. [2003]). Expression (4) describing the inflationary effect in terms of the covariance between local growth rate and relative abundance can be viewed as a component of fitness that selection can act upon. If a behavioral variant arises that increased the match between the spatial distribution of that variant and its temporarily greater local growth rate, that variant would have a selective advantage. This is one way of describing the fitness advantage of habitat selection, a point illustrated by Altenberg (2012) in the context of the evolution of dispersal. Temporal autocorrelation structure relevant to the inflationary effect is known to influence dispersal evolution (Travis 2001), and positive autocorrelations typically favor habitat selection fostering use of temporarily high-quality sites, which can promote metapopulation persistence (Schmidt 2004).

Conclusions

This paper is an invited contribution to a special feature of *The American Naturalist* on the theme of neglected and misunderstood mathematical theories in ecology. We hope to have illustrated that work on the inflationary effect clarifies and extends the intuition of ecologists about the role of spatiotemporal variation in fitness—in interplay with dispersal—in promoting the regional persistence of species. These ideas have a long history and are entrenched in ecological thinking. For example, Andrewartha and Birch (1954, p. 657) remarked, "A natural population occupying any considerable area will be made up of a number of . . . local populations or colonies. In different localities the trends may be going in different directions at the same time." den Boer (1981) studied differences in ground beetle fluctuations over 35 years and showed that the beetle *Pterostichus versicolor* fluctuated asynchronous across 10 locations without

local extinction, while the beetle *Calathus melanocephalus* fluctuated synchronously, with multiple local extinctions. Gotelli (2008, p. 96) pointed out the link between persistent and spatiotemporal fluctuations in de Boer's study, noting that "at any point in time, some populations were increasing in size and acting as source populations that prevented the extinction of other, declining sink populations." Presciently, den Boer was thinking about the nature of spatiotemporal heterogeneity and its effects when he developed his idea of risk spreading (den Boer 1968), which Andrewartha and Birch lauded, noting, "The concept of spreading risk recognized the importance of dispersal with the natural population that enables individuals to colonize new localities" (Andrewartha and Birch 1984, p. 175). They extensively quote den Boer (1981, p. 39), who suggests, "The survival time of composite populations uninterruptedly inhabiting large and heterogeneous areas, highly depends on the extent to which the numbers fluctuate unequally in the different subpopulations." In other words, population persistence at broad scales may rest on the interplay of dispersal and spatiotemporal variation in fitness.

One of the lessons to emerge from the recent pandemic is that the issues of spatiotemporal heterogeneity in fitness is not only relevant for ecologists understanding natural populations but also for policy makers dealing with the spread of infectious disease. Pathogen eradication is extremely rare among human pathogens, a fact we believe occurs in part because of the large heterogeneities present at the scale of human societies that allow persistence, much in the way that den Boer, Andrewartha, and Birch discussed for natural populations of insects. We submit that ignorance of these emergent effects possibly contributed to the failure of governmental control of the COVID-19 pandemic in its early phases in many parts of the globe. In some circumstances, human decisions may have even generated spatiotemporal variability that exacerbated pathogen spread. There was, for example, in the early phases of the pandemic, a block-by-block control strategy in New York (Guarino 2020) and local whack-a-mole strategies in the United Kingdom (BBC 2020). Such uncoordinated interventions—paired with continued movement of asymptomatic infectious individuals among locations (Sah et al. 2021)—likely contributed (to a degree not yet known) to the pervasive failure of control. Failure to recognize the epidemiological consequences of spatiotemporal variability and its potential to boost abundances through the inflationary effect perhaps fostered a great deal of human suffering.

The throughline connecting Andrewartha and Birch with COVID-19 is the role of spatiotemporal heterogeneity in population growth and persistence. Despite recognizing its importance for decades, a new generation of empirical research is needed to establish how widespread the inflationary effect is in nature (see table 1 for the necessary features), and further theoretical studies of its role in ecology and evolution are important desiderata for future research. The quantitative theory we present can help describe how important the inflationary effect is for understanding the dynamics of species and the structure of communities and also for the health of human societies in the face of emerging pathogens.

Acknowledgments

We thank associate editor Rachel Germain and Sebastian Schreiber for inviting us to explore these connections and for great suggestions for improving the rigor and clarity of the ideas. We also thank Michael Barfield and three anonymous reviewers whose perceptive and thoughtful feedback greatly improved the manuscript. This work was supported by National Science Foundation grants DMS-2327799, DMS-2327798, DMS-2327797, and DEB-1655555 as well as US Department of Agriculture awards 2023-67015-40544 and 2017-67013-26870 granted as part of the joint NIFA-NSF-NIH Ecology and Evolution of Infectious Disease program. R.D.H. is supported by the University of Florida Foundation, and A.G. is supported by the Liber Ero Chair for Biodiversity Conservation.

Statement of Authorship

Conceptualization: N.K., R.D.H.; funding acquisition: N.K., N.W.R., R.D.H.; model development, analysis, coding, and visualization: N.K.; writing (original draft): all authors; writing (review and editing): all authors.

Data and Code Availability

Code to reproduce the figures here and in the supplementary material is available on Zenodo (https://doi.org/10.5281/zenodo.13928922; Kortessis 2024).

Literature Cited

Akçakaya, H. R., G. Mills, and C. P. Doncaster. 2007. The role of metapopulations in conservation. Pages 64–84 *in* D. W. Macdonald and K. Service, eds. Key topics in conservation biology. Vol. 1. Blackwell, Oxford.

Altenberg, L. 2012. The evolution of dispersal in random environments and the principle of partial control. Ecological Monographs 82:297–333.

Amarasekare, P. 2003. Competitive coexistence in spatially structured environments: a synthesis. Ecology Letters 6:1109–1122.

Andrewartha, H. G., and L. C. Birch. 1954. The distribution and abundance of animals. University of Chicago Press, Chicago.

———. 1984. The ecological web: more on the distribution and abundance of animals. University of Chicago Press, Chicago.

Barfield, M., M. E. Orive, and R. D. Holt. 2015. The role of pathogen shedding in linking within- and between-host pathogen dynamics. Mathematical Biosciences 270:249–262.

BBC. 2020. Boris Johnson's "Weston lockdown" claims criticised. BBC, June 30.

Bell, G., and A. Gonzalez. 2011. Adaptation and evolutionary rescue in metapopulations experiencing environmental deterioration. Science 332:1327–1330.

Bellard, C., C. Marino, and F. Courchamp. 2022. Ranking threats to biodiversity and why it doesn't matter. Nature Communications 13:2616.

Benaïm, M., C. Lobry, T. Sari, and É. Strickler. 2023. Untangling the role of temporal and spatial variations in persistence of populations. Theoretical Population Biology 154:1–26.

Berestycki, H., B. Desjardins, J. S. Weitz, and J.-M. Oury. 2023. Epidemic modeling with heterogeneity and social diffusion. Journal of Mathematical Biology 86:60.

Blasius, B., L. Rudolf, G. Weithoff, U. Gaedke, and G. F. Fussmann. 2020. Long-term cyclic persistence in an experimental predator–prey system. Nature 577:226–230.

Bolker, B., and S. W. Pacala. 1997. Using moment equations to understand stochastically driven spatial pattern formation in ecological systems. Theoretical Population Biology 52:179–197.

Bolker, B. M., and B. T. Grenfell. 1996. Impact of vaccination on the spatial correlation and persistence of measles dynamics. Proceedings of the National Academy of Sciences of the USA 93:12648–12653.

Brook, B. W., N. S. Sodhi, and C. J. A. Bradshaw. 2008. Synergies among extinction drivers under global change. Trends in Ecology and Evolution 23:453–460.

Chesson, P. L. 1981. Models for spatially distributed populations: the effect of within-patch variability. Theoretical Population Biology 19:288–325.

———. 1985. Coexistence of competitors in spatially and temporally varying environments: a look at the combined effects of different sorts of variability. Theoretical Population Biology 28:263–287.

Cliff, A. D., P. Haggett, and M. R. Smallman-Raynor. 2000. Island epidemics. Oxford University Press, Oxford.

den Boer, P. J. 1968. Spreading of risk and stabilization of animal numbers. Acta Biotheoretica 18:165–194.

———. 1981. On the survival of populations in a heterogeneous and variable environment. Oecologia 50:39–53.

Driscoll, D. A., and D. B. Lindenmayer. 2009. Empirical tests of metacommunity theory using an isolation gradient. Ecological Monographs 79:485–501.

Duncan, A. B., A. Gonzalez, and O. Kaltz. 2013. Stochastic environmental fluctuations drive epidemiology in experimental host–parasite metapopulations. Proceedings of the Royal Society B 280:20131747.

Eksin, C., M. Ndeffo-Mbah, and J. S. Weitz. 2021. Reacting to outbreaks at neighboring localities. Journal of Theoretical Biology 520:110632.

Fox, J. W., D. Vasseur, M. Cotroneo, L. Guan, and F. Simon. 2017. Population extinctions can increase metapopulation persistence. Nature Ecology and Evolution 1:1271–1278.

Gaggiotti, O. E., and I. Hanski. 2004. 14 - Mechanisms of population extinction. Pages 337–366 *in* I. Hanski and O. E. Gaggiotti, eds. Ecology, genetics and evolution of metapopulations. Elsevier Academic Press, Burlington, MA.

Gonzalez, A., and R. D. Holt. 2002. The inflationary effects of environmental fluctuations in source–sink systems. Proceedings of the National Academy of Sciences of the USA 99:14872–14877.

Gonzalez, A., J. H. Lawton, F. S. Gilbert, T. M. Blackburn, and I. Evans-Freke. 1998. Metapopulation dynamics, abundance, and distribution in a microecosystem. Science 281:2045–2047.

Gotelli, N. J. 2008. A primer of ecology. 4th ed. Oxford University Press, Oxford.

Gouhier, T. C., F. Guichard, and A. Gonzalez. 2010. Synchrony and stability of food webs in metacommunities. American Naturalist 175:E16–E34.

Gravel, D., F. Massol, and M. A. Leibold. 2016. Stability and complexity in model meta-ecosystems. Nature Communications 7:12457.

Guarino, B. 2020. New York's block-by-block lockdowns are curbing covid-19. But residents aren't pleased. Washington Post, November 8.

Hansen, B. B., V. Grøtan, I. Herfindal, and A. M. Lee. 2020. The Moran effect revisited: spatial population synchrony under global warming. Ecography 43:1591–1602. https://doi.org/10.1111/ecog.04962.

Hansen, B. B., Å. Ø. Pedersen, B. Peeters, M. Le Moullec, S. D. Albon, I. Herfindal, B.-E. Sæther, V. Grøtan, and R. Aanes. 2019. Spatial heterogeneity in climate change effects decouples the long-term dynamics of wild reindeer populations in the high Arctic. Global Change Biology 25:3656–3668.

Hanski, I. 1997. Metapopulation dynamics: from concepts and observations to predictive models. Pages 69–91 *in* I. Hanski and M. E. Gilpin, eds. Metapopulation biology. Academic Press, San Diego.

———. 1998. Metapopulation dynamics. Nature 396:41–49.

Hanski, I., and O. Gaggiotti. 2004. Metapopulation biology: past, present, and future. Pages 3–22 *in* I. Hanski and O. E. Gaggiotti, eds. Ecology, genetics and evolution of metapopulations. Elsevier Academic Press, Burlington, MA.

Hanski, I., T. Mononen, and O. Ovaskainen. 2011. Eco-evolutionary metapopulation dynamics and the spatial scale of adaptation. American Naturalist 177:29–43.

Harrison, S., and J. F. Quinn. 1989. Correlated environments and the persistence of metapopulations. Oikos 56:293–298.

Hassell, M. P., H. N. Comins, and R. M. Mayt. 1991. Spatial structure and chaos in insect population dynamics. Nature 353:255–258.

Hassell, M. P., and R. M. May. 1988. Spatial heterogeneity and the dynamics of parasitoid-host systems. Annales Zoologici Fennici 25:55–61.

Hastings, A. 1977. Spatial heterogeneity and the stability of predator-prey systems. Theoretical Population Biology 12:37–48.

———. 1980. Disturbance, coexistence, history, and competition for space. Theoretical Population Biology 18:363–373.

Holmes, E. E., M. A. Lewis, J. E. Banks, and R. R. Veit. 1994. Partial differential equations in ecology: spatial interactions and population dynamics. Ecology 75:17–29.

Holt, G., and P. Chesson. 2016. Scale-dependent community theory for streams and other linear habitats. American Naturalist 188: E59–E73.

Holt, R. D. 1985. Population dynamics in two-patch environments: some anomalous consequences of an optimal habitat distribution. Theoretical Population Biology 28:181–208.

———. 1993. Ecology at the mesoscale: the influence of regional processes on local communities. Pages 77–88 *in* R. E. Ricklefs and D. Schluter, eds. Species diversity in ecological communities. University of Chicago Press, Chicago.

———. 1997. From metapopulation dynamics to community structure: some consequences of spatial heterogeneity. Pages 149–164 *in* I. Hanski and M. E. Gilpin, eds. Metapopulation biology. Academic Press, San Diego.

Holt, R. D., M. Barfield, and A. Gonzalez. 2003. Impacts of environmental variability in open populations and communities: "inflation" in sink environments. Theoretical Population Biology 64:315–330.

Holt, R. D., and T. H. Keitt. 2000. Alternative causes for range limits: a metapopulation perspective. Ecology Letters 3:41–47.

Hoopes, M. F., R. D. Holt, and M. Holyoak. 2005. The effects of spatial processes on two species interactions. Pages 35–67 *in* M. Holyoak, M. A. Leibold, and R. D. Holt, eds. Metacommunities: spatial dynamics and ecological communities. University of Chicago Press, Chicago.

Huffaker, C. 1958. Experimental studies on predation: dispersion factors and predator-prey oscillations. Hilgardia 27:343–383.

Ingvarsson, P. 2002. A metapopulation perspective on genetic diversity and differentiation in partially self-fertilizing plants. Evolution 56:2368–2373.

Johnson, E. C., and A. Hastings. 2023. Coexistence in spatiotemporally fluctuating environments. Theoretical Ecology 16:59–92.

Katriel, G. 2022. Dispersal-induced growth in a time-periodic environment. Journal of Mathematical Biology 85:24.

Keddy, P. A. 1982. Population ecology on an environmental gradient: *Cakile edentula* on a sand dune. Oecologia 52:348–355.

Keeling, M. J., H. B. Wilson, and S. W. Pacala. 2000. Reinterpreting space, time lags, and functional responses in ecological models. Science 290:1758–1761.

Kelly, L. T., A. F. Bennett, M. F. Clarke, and M. A. McCarthy. 2015. Optimal fire histories for biodiversity conservation. Conservation Biology 29:473–481.

Kortessis, N. 2024. kortessis/Asynchrony-and-Inflationary-Effect: v1.0.1. Zenodo, https://doi.org/10.5281/zenodo.13928923.

Kortessis, N., M. W. Simon, M. Barfield, G. E. Glass, B. H. Singer, and R. D. Holt. 2020. The interplay of movement and spatiotemporal variation in transmission degrades pandemic control. Proceedings of the National Academy of Sciences of the USA 117:30104–30106.

Leibold, M. A., and J. M. Chase. 2018. Metacommunity ecology. Princeton University Press, Princeton, NJ.

Leibold, M. A., F. J. Rudolph, F. G. Blanchet, L. De Meester, D. Gravel, F. Hartig, P. Peres-Neto, L. Shoemaker, and J. M. Chase. 2022. The internal structure of metacommunities. Oikos 2022: 08618.

Levin, S. A. 1974. Dispersion and population interactions. American Naturalist 108:207–228.

Levins, R. 1969. Some demographic and genetic consequences of environmental heterogeneity for biological control. Bulletin of the Entomological Society of America 15:237–240.

———. 1970. Extinction. Lecture Notes in Biomathematics 2:75–107.

Long, Z. T., O. L. Petchey, and R. D. Holt. 2007. The effects of immigration and environmental variability on the persistence of an inferior competitor. Ecology Letters 10:574–585.

Loreau, M., N. Mouquet, and A. Gonzalez. 2003. Biodiversity as spatial insurance in heterogeneous landscapes. Proceedings of the National Academy of Sciences of the USA 100:12765–12770.

Lu, M. 2021. Complex relationships between beta diversity and dispersal in meta-community models. Ecography 44:1769–1780.

Matthews, D. P., and A. Gonzalez. 2007. The inflationary effects of environmental fluctuations ensure the persistence of sink metapopulations. Ecology 88:2848–2856.

May, R. M. 1972. Limit cycles in predator-prey communities. Science 177:900–902.

Melbourne, B. A., H. V. Cornell, K. F. Davies, C. J. Dugaw, S. Elmendorf, A. L. Freestone, R. J. Hall, et al. 2007. Invasion in a heterogeneous world: resistance, coexistence or hostile takeover? Ecology Letters 10:77–94.

Noss, R. F. 2018. Fire ecology of Florida and the southeastern coastal plain. University Press of Florida, Gainsville, FL.

Olivieri, I., Y. Michalakis, and P.-H. Gouyon. 1995. Metapopulation genetics and the evolution of dispersal. American Naturalist 146:202–228.

Ovaskainen, O., and I. Hanski. 2004. Metapopulation dynamics in highly fragmented landscapes. Pages 73–103 *in* I. Hanski and O. E. Gaggiotti, eds. Ecology, genetics and evolution of metapopulations. Elsevier Academic Press, Burlington, MA.

Peniston, J. H., G. A. Backus, M. L. Baskett, R. J. Fletcher, and R. D. Holt. 2024. Ecological and evolutionary consequences of temporal variation in dispersal. Ecography 2024:e06699.

Petchey, O. L., A. Gonzalez, and H. B. Wilson. 1997. Effects on population persistence: the interaction between environmental noise colour, intraspecific competition and space. Proceedings of the Royal Society B 264:1841–1847.

Pillai, P., A. Gonzalez, and M. Loreau. 2011. Metacommunity theory explains the emergence of food web complexity. Proceedings of the National Academy of Sciences of the USA 108:19293–19298.

Poethke, H. J., W. W. Weisser, and T. Hovestadt. 2010. Predator-induced dispersal and the evolution of conditional dispersal in correlated environments. American Naturalist 175:577–586.

Pulliam, H. R. 1988. Sources, sinks, and population regulation. American Naturalist 132:652–661.

Reuman, D. C., M. C. N. Castorani, K. C. Cavanaugh, L. W. Sheppard, J. A. Walter, and T. W. Bell. 2023. How environmental drivers of spatial synchrony interact. Ecography 2023:e06795.

Roy, M., R. D. Holt, and M. Barfield. 2005. Temporal autocorrelation can enhance the persistence and abundance of metapopulations comprised of coupled sinks. American Naturalist 166:246–261.

Ruktanonchai, N. W., J. R. Floyd, S. Lai, C. W. Ruktanonchai, A. Sadilek, P. Rente-Lourenco, X. Ben, et al. 2020. Assessing the impact of coordinated COVID-19 exit strategies across Europe. Science 369:1465–1470.

Runge, J. P., M. C. Runge, and J. D. Nichols. 2006. The role of local populations within a landscape context: defining and classifying sources and sinks. American Naturalist 167:925–938.

Sah, P., M. C. Fitzpatrick, C. F. Zimmer, E. Abdollahi, L. Juden-Kelly, S. M. Moghadas, B. H. Singer, and A. P. Galvani. 2021. Asymptomatic SARS-CoV-2 infection: a systematic review and meta-analysis. Proceedings of the National Academy of Sciences of the USA 118:e2109229118.

Schmidt, K. A. 2004. Site fidelity in temporally correlated environments enhances population persistence. Ecology Letters 7:176–184.

Schreiber, S. J. 2010. Interactive effects of temporal correlations, spatial heterogeneity and dispersal on population persistence. Proceedings of the Royal Society B 277:1907–1914.

———. 2025. Partitioning the impacts of spatial-temporal variation in demography and dispersal on metapopulation growth rates. American Naturalist (forthcoming).

Shanafelt, D. W., U. Dieckmann, M. Jonas, O. Franklin, M. Loreau, and C. Perrings. 2015. Biodiversity, productivity, and the spatial insurance hypothesis revisited. Journal of Theoretical Biology 380:426–435.

Shoemaker, L. G., L. M. Hallett, L. Zhao, D. C. Reuman, S. Wang, K. L. Cottingham, R. J. Hobbs, et al. 2022. The long and the short of it: mechanisms of synchronous and compensatory dynamics across temporal scales. Ecology 103:e3650.

Stier, A. C., A. O. Shelton, J. F. Samhouri, B. E. Feist, and P. S. Levin. 2020. Fishing, environment, and the erosion of a population portfolio. Ecosphere 11:e03283.

Thompson, P. L., and A. Gonzalez. 2017. Dispersal governs the reorganization of ecological networks under environmental change. Nature Ecology and Evolution 1:1–8.

Thompson, P. L., B. Rayfield, and A. Gonzalez. 2017. Loss of habitat and connectivity erodes species diversity, ecosystem functioning, and stability in metacommunity networks. Ecography 40:98–108.

Tilman, D. 1994. Competition and biodiversity in spatially structured habitats. Ecology 75:2–16.

Travis, J. M. J. 2001. The color of noise and the evolution of dispersal. Ecological Research 16:157–163.

Van Horne, B. 1983. Density as a misleading indicator of habitat quality. Journal of Wildlife Management 47:893–901.

Vasseur, D. A., and J. W. Fox. 2009. Phase-locking and environmental fluctuations generate synchrony in a predator–prey community. Nature 460:1007–1010.

Wang, S., and F. Altermatt. 2019. Metapopulations revisited: the area-dependence of dispersal matters. Ecology 100:e02792.

Wang, Q., and H. Wu. 2022. There exists the "smartest" movement rate to control the epidemic rather than "city lockdown." Applied Mathematical Modelling 106:696–714.

Wieczynski, D. J., and D. A. Vasseur. 2016. Environmental fluctuations promote intraspecific diversity and population persistence via inflationary effects. Oikos 125:1173–1181.

Williams, P. D., and A. Hastings. 2011. Paradoxical persistence through mixed-system dynamics: towards a unified perspective of reversal behaviours in evolutionary ecology. Proceedings of the Royal Society B 278:1281–1290.

Wilson, D. S. 1992. Complex interactions in metacommunities, with implications for biodiversity and higher levels of selection. Ecology 73:1984–2000.

Winter, A. K., B. Lambert, D. Klein, P. Klepac, T. Papadopoulos, S. Truelove, C. Burgess, et al. 2022. Feasibility of measles and rubella vaccination programmes for disease elimination: a modelling study. Lancet Global Health 10:e1412–e1422.

Zhang, B., S. Liang, G. Wang, C. Zhang, C. Chen, M. Zou, W. Shen, et al. 2021. Synchronized nonpharmaceutical interventions for the control of COVID-19. Nonlinear Dynamics 106:1477–1489.

References Cited Only in the Online Enhancements

Casella, G., and R. J. Berger. 2001. Statistical inference. Cengage Learning, Boston.

Ghosh, S., L. W. Sheppard, M. T. Holder, T. D. Loecke, P. C. Reid, J. D. Bever, and D. C. Reuman. 2020. Copulas and their potential for ecology. Advances in Ecological Research 62:409–468.

Kortessis, N., and P. Chesson. 2019. Germination variation facilitates the evolution of seed dormancy when coupled with seedling competition. Theoretical Population Biology 130:60–73.

———. 2021. Character displacement in the presence of multiple trait differences: evolution of the storage effect in germination and growth. Theoretical Population Biology 140:54–66.

Schreiber, S. J., A. Hening, and D. H. Nguyen. 2023. Coevolution of patch selection in stochastic environments. American Naturalist 202:122–139.

Associate Editor: Rachel M. Germain
Editor: Volker H. W. Rudolf

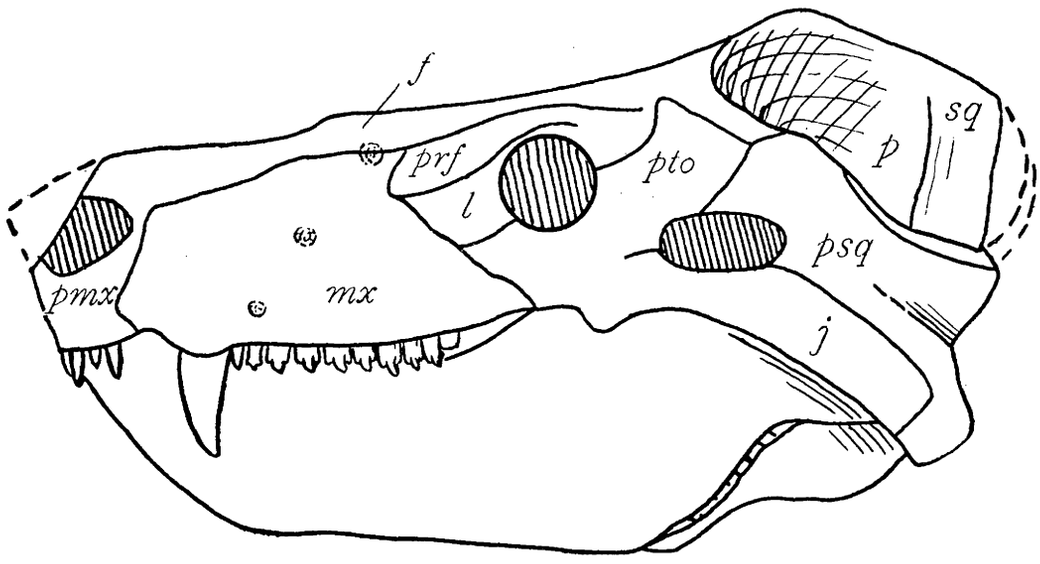

"Perhaps the greatest interest excited in the morphology of the Permian reptiles of the order Pelycosauria centers about the development of the temporal and quadrate regions as they seem at present to afford the most direct phylogenetic evidence of the origin of mammals." Figured: "Cynognathus crateronotus. Side view of skull. *pmx*, premaxillary; *mx*, maxillary; *f*, frontal; *prf*, prefrontal; *l*, lachrymal; *pto*, postorbital; *p*, parietal; *sq*, squamosal; *psq*, prosquamosal; *j*, jugal. After Seeley." From "The Structure and Relationships of the American Pelycosauria" by E. C. Case (*The American Naturalist*, 1903, 37:85–102).

Supplemental Material (not copyedited or formatted) for: Nicholas Kortessis, Gregory Glass, Andrew Gonzalez, Nick W. Ruktanonchai, Margaret W. Simon, Burton Singer, Robert D. Holt. 2025. "Metapopulations, the Inflationary Effect, and Consequences for Public Health."
The American Naturalist 205(3). DOI: https://doi.org/10.1086/733896.

Online Supplement: Metapopulations, the inflationary effect, and consequences for public health

Nicholas Kortessis[1,*]
Gregory Glass[2,3]
Andrew Gonzalez[4]
Nick W. Ruktanonchai[5]
Margaret W. Simon[6]
Burton Singer[3]
Robert D. Holt[6]

1. Department of Biology, Wake Forest University, Winston-Salem, NC 27106;
2. Department of Geography, University of Florida, Gainesville, FL, 32611;
3. Emerging Pathogens Institute, University of Florida, Gainesville, FL, 32610;
4. Department of Biology, McGill University, Montreal, Quebec, Canada H3A 1B1
5. Department of Population Health Sciences, Virginia Polytechnic University, Blacksburg, VA, 24061;
6. Department of Biology, University of Florida, Gainesville, FL, 32611;
∗ Corresponding author; e-mail: kortessn@wfu.edu.
Journal: *The American Naturalist*

Supplemental Material (not copyedited or formatted) for: Nicholas Kortessis, Gregory Glass, Andrew Gonzalez, Nick W. Ruktanonchai, Margaret W. Simon, Burton Singer, Robert D. Holt. 2025. "Metapopulations, the Inflationary Effect, and Consequences for Public Health."
The American Naturalist 205(3). DOI: https://doi.org/10.1086/733896.

Contents

Supplemental Material (not copyedited or formatted) for: Nicholas Kortessis, Gregory Glass, Andrew Gonzalez, Nick W. Ruktanonchai, Margaret W. Simon, Burton Singer, Robert D. Holt. 2025. "Metapopulations, the Inflationary Effect, and Consequences for Public Health."
The American Naturalist 205(3). DOI: https://doi.org/10.1086/733896.

S1 Formalizing spatiotemporal variation

Here we provide a mathematical justification for the expressions of different variance components.

We begin with a set of data $F(t,x)$ that can be indexed by time t and spatial location x. Assume for simplicity that this data is measured without error, such that there is no need to partition out measurement or sampling error. To calculate the variance in this data, and moreover to break that variance into different components, we need to introduce the conditional data

$$F|x \tag{S1}$$

and

$$F|t. \tag{S2}$$

The data $F|x$ gives the outcomes across time at a specified location x. In essence, it is the distribution of conditions in time at location x. Similarly, $F|t$ gives the conditions across space at particular time t.

We can calculate the variance in $F(t,x)$ using the law of total variance such that

$$\text{Var}(F) = E_x[\text{Var}_t(F|x)] + \text{Var}_x(E_t[F|x]), \tag{S3}$$

where $E_x[\cdot]$ and $E_t[\cdot]$ are spatial and temporal averages, respectively, and $\text{Var}_x(\cdot)$ and $\text{Var}_t(\cdot)$ are spatial and temporal variances, respectively.

To partition this variation into space, time, and spatiotemporal components, we introduce the concepts of the temporal mean field and the spatial mean field. A temporal mean field model is one in which conditions that vary over time are represented by their mean. A model of the temporal mean field includes spatial variation but any temporal variation is represented simply by the mean. Let $\tilde{F}_x := E_t[F|x]$ be the distribution of fitness-affecting conditions present in such a model. These conditions have variance

$$\sigma_S^2 = \text{Var}_x(\tilde{F}_x) = \text{Var}_x(E_t[F|x]), \tag{S4}$$

which is entirely comprised of spatial variation and so represents "spatial-only" variation.

A spatial mean field model is one in which conditions that vary across space are represented by their mean. A model of the spatial mean field includes temporal variation but any spatial variation is represented simply by the mean. Let $\bar{F}_t := E_x[F|t]$ be the distribution of fitness-affecting conditions present in such a model. These conditions have variance

$$\sigma_T^2 = \text{Var}_t(\bar{F}_t) = \text{Var}_t(E_x[F|t]), \tag{S5}$$

which is entirely comprised of temporal variation and so represents "temporal-only" variation.

Supplemental Material (not copyedited or formatted) for: Nicholas Kortessis, Gregory Glass, Andrew Gonzalez, Nick W. Ruktanonchai, Margaret W. Simon, Burton Singer, Robert D. Holt. 2025. "Metapopulations, the Inflationary Effect, and Consequences for Public Health."
The American Naturalist 205(3). DOI: https://doi.org/10.1086/733896.

Substituting (S4) into (S3) and adding and subtracting σ_T^2 yields

$$\mathrm{Var}(F) = E_x[\mathrm{Var}_t(F|x)] + \mathrm{Var}_x(E_t[F|x]) \tag{S6}$$

$$= E_x[\mathrm{Var}_t(F|x)] - \mathrm{Var}_t(E_x[F|t]) + \sigma_S^2 + \sigma_T^2 \tag{S7}$$

$$\mathrm{Var}(F) = \sigma_S^2 + \sigma_T^2 + \sigma_{ST}^2, \tag{S8}$$

where in the last line we have defined $\sigma_{ST}^2 = E_x[\mathrm{Var}_t(F|x)] - \mathrm{Var}_t(E_x[F|t])$ as the magnitude of spatio-temporal variation. Spatio-temporal variation is the variation in F that remains after accounting for spatial-only and temporal-only variation.

S1.1 Spatiotemporal heterogeneity despite synchrony

Spatiotemporal heterogeneity does not imply asynchrony (although asynchrony implies spatiotemporal heterogeneity). One way to see this is to formalize the example of temperature in different water bodies. Let $F_{x,t}$ be the temperature at time t in water body x. A model to describe temperature is

$$F_{x,t} = \mu + S_x + Z_x X_t, \tag{S9}$$

where S_x is a random variable describing spatial variability and X_t is the random variable describing temporal variation. Without loss of generality, assume $E[S_x] = 0$ and $E[X_t] = 0$. As such, the parameter μ is a grand mean across space and time. The variable Z_x is a given location's sensitivity to temporal variation. The model given by eqn. (S9) is essentially a linear regression model of spatio-temporally structured data with environmental conditions $F_{x,t}$ regressed against conditions over time, X_t, with random intercepts (S_x) and random slopes (Z_x) for differential spatial locations.

The variance partition in equation (S8) shows contributions from each component. The pure spatial variance for model (S9) is $\sigma_S^2 = \mathrm{Var}(S_x)$. The pure temporal variance is $\sigma_T^2 = E[Z_x]^2\mathrm{Var}(X_t)$. The spatiotemporal variance is $\sigma_{ST}^2 = \mathrm{Var}(X_t)\mathrm{Var}(Z_x)$. Thus, spatiotemporal variability is present provided locations are differently sensitive to a common environmental factor (i.e., $\mathrm{Var}(Z_x) > 0$). In a linear regression framework, there is spatiotemporal heterogeneity provided a random slopes model fits nonzero variance of the slope distribution.

This model can include perfectly synchronized fluctuations across space. To see how, consider two locations denoted A and B. The correlation between $F_{A,t}$ and $F_{B,t}$ is $\mathrm{sgn}(z_A z_B)$, that is, the sign of the product of the slopes in the two locations. When the slopes are of the same sign, the correlation is 1. When the slopes are different signs, the correlation is -1. Hence, this model includes the case of complete synchrony whenever the distribution of Z_x has nonzero variance and exists on the nonnegative real numbers.

Supplemental Material (not copyedited or formatted) for: Nicholas Kortessis, Gregory Glass, Andrew Gonzalez, Nick W. Ruktanonchai, Margaret W. Simon, Burton Singer, Robert D. Holt. 2025. "Metapopulations, the Inflationary Effect, and Consequences for Public Health."
The American Naturalist 205(3). DOI: https://doi.org/10.1086/733896.

S2 Stochastic metapopulation model

Here we provide a mathematical overview of the metapopulation model with (patch-level) demographic stochasticity. This model is conceptually similar to the traditional metapopulation model as introduced by Levins, but follows a finite number of patches. Given the finite number of patches, we must deal with the metapopulation analogue to demographic stochasticity, which is random deviations in extinction and colonization from large-scale averages.

The model is a discrete-time Markov chain for n patches, and it models the occupancy of a all patches as denoted with the time-dependent vector $\mathbf{O}(t) = (O_1(t), O_2(t), \ldots, O_n(t))^T$. Each $O_i(t)$ can be either 0, corresponding to an empty patch, or 1, corresponding to an occupied patch. Occupancy changes states (or stays in the same state) with extinction and colonization probabilities, E_i and $C_i(t)$, respectively. To formalize the model, a typical approach is to write the transition probabilities for all patches. To do so, define P_t^i as

$$P_t^i(a,b) := P\Big(O_i(t+\Delta t) = b | O_i(t) = a\Big), \tag{S10}$$

the probability that patch i in state a at time t transitions to state b in the time interval $(t, t+\Delta t]$. Given the extinction and colonization probabilities above, we have

$$P_t^i(0,0) = 1 - C_i(t) \qquad P_t^i(0,1) = C_i(t) \tag{S11}$$

$$P_t^i(1,0) = E_i(t) \qquad P_t^i(1,1) = 1 - E_i(t). \tag{S12}$$

Given that we are only interested in illuminating the consequences of asynchrony, we keep the assumptions of the model simple. In particular, we assume that all patches are the same size and are equally connected, implying global dispersal. These assumptions correspond to the assumptions developed initially by Levins for the first metapopulation model in continuous-time. We set

$$E_i = 1 - \exp(-e\Delta t) \tag{S13}$$

for all patches, where e is the infinitesimal rate of extinction, and Δt is a small unit of time. This model of extinction has the typical biological interpretation that all patches are effectively identical with respect to factors that influence extinction, and corresponds to an extinction rate of e in the limit as $\Delta t \to 0$.

We also assume that the probability that an unoccupied patch stays unoccupied is

$$1 - C_i(t) = \exp\big(-cP(t)\Delta t\big), \tag{S14}$$

such that the colonization probability is

$$C_i(t) = 1 - \exp\big(-cP(t)\Delta t\big). \tag{S15}$$

This colonization model implies that colonization rates depend on the occupancy on the landscape and occur at infinitesimal rate $cP(t)$. Indeed, in the limit as the time interval becomes very

Supplemental Material (not copyedited or formatted) for: Nicholas Kortessis, Gregory Glass, Andrew Gonzalez, Nick W. Ruktanonchai, Margaret W. Simon, Burton Singer, Robert D. Holt. 2025. "Metapopulations, the Inflationary Effect, and Consequences for Public Health."
The American Naturalist 205(3). DOI: https://doi.org/10.1086/733896.

small, this discrete-time model converges on the continuous-time metapopulation model (1) of the main text.

The conditional transition probabilities (S11)-(S12) alone are not enough to specify this model. The full model requires a statement about the *joint probability* of extinction and colonization across patches. We need to stipulate whether transition probabilities act independently across patches or are correlated in some way. For example, if there is a 50% chance of extinction, the joint distribution tells us whether the 50% of times when a patch changes state occur at the same time as other patches, different times as other patches, or without respect to what happens in any other patch.

A typical assumption is that extinction probabilities are independent across patches (and the same for colonization probabilities). In this special case of independence, one can simply model *how many* patches go extinct in one time period using the binomial distribution. In this model, the number of extinctions is $\text{Binom}(\sum_i O_i(t), E_i)$. Biologically, the binomial distribution implies that the factors influencing extinction in one patch at one time are completely unrelated to those in any other patch across space. That may very well be true, but is a specific case of a broader set of possibilities.

To model the broader range of possibilities, we use a latent variable approach that describes a hypothetical environmental variable affecting extinction and colonization in each patch. We then use properties of the extinction and colonization probabilities to create a reaction norm relating local environmental characteristics to extinction or colonization events.

Note that while this works for discrete-time models, correlated events can be described in true continuous-time as correlated times to extinction. However, such a mathematical description is beyond the scope of this paper. The approach here is sufficient to illustrate the point.

To model correlated events, let $X_i(t)$ be the environmental conditions in patch i at time t. For simplicity for modeling correlations between variables, we assume that $X_i(t)$ is a standard normal random variable that is i.i.d. (independent and identically distributed) over time; hence, $X_i(t) \overset{\text{iid}}{\sim} \mathcal{N}(0,1)$ for all i. To include correlations between conditions in patches across space, we collect all individual environmental variables as a multivariate collection $\mathbf{X}(t) = (X_1(t), X_2(t), \ldots, X_n(t))^T$ that follows a multivariate normal with zero mean and covariance matrix Σ. Because all the marginal variables are standard normal, Σ has values of 1 for all diagonal elements and therefore takes the interpretation of a correlation matrix. Again, for simplicity, we assume this correlation matrix has the simple structure where $\text{Corr}(X_i(t), X_j(t)) = \rho$, for all $i \neq j$. Written succinctly,

$$\mathbf{X}(t) \overset{\text{iid}}{\sim} \mathcal{N}_n\Big(\mathbf{0}, \Sigma = \rho\mathbf{1}\cdot\mathbf{1}^T + (1-\rho)\mathbf{I}\Big), \tag{S16}$$

where $\mathbf{1}$ is an n-length column vector of ones.

Correlations take values between -1 and 1. However, given that the correlation applies to all possible pairs of patches, the multivariate normal will not permit ρ near -1 when $n > 2$. Indeed,

Supplemental Material (not copyedited or formatted) for: Nicholas Kortessis, Gregory Glass, Andrew Gonzalez, Nick W. Ruktanonchai, Margaret W. Simon, Burton Singer, Robert D. Holt. 2025. "Metapopulations, the Inflationary Effect, and Consequences for Public Health."
The American Naturalist 205(3). DOI: https://doi.org/10.1086/733896.

larger n restricts the range of permissible values of ρ based on the requirement that $\mathbf{\Sigma}$ be positive semi-definite. To satisfy this restriction, we only consider ρ values between 0 and 1.

To translate this environment into an extinction (or colonization) event, we convert the environmental variables, $\mathbf{X}(t)$, into multivariate Bernoulli random variables using copulas. Copulas are used to create correlated random variables in cases where the marginals are of different distributional form or more generally where the multivariate distribution has no known analytical form. Copulas and their use in ecology are discussed by Ghosh et al. (2020). For examples of the use of copulas for questions of life history evolution in plant communities, see Kortessis and Chesson (2018, 2021).

Here, the goal is to have a multivariate distribution of extinction events at each time step under the provision that each marginal distribution has the probability E_i of an extinction event in time t. Thus, we need a random variable

$$Y_i(t) = \begin{cases} 1 & \text{with probability } E_i \\ 0 & \text{with probability } 1 - E_i \end{cases}, \tag{S17}$$

where $Y_i(t) = 1$ means that a population i that was occupied in time t goes extinct in time $t+1$.

The transformation for $Y_i(t)$ from $X_i(t)$ is

$$Y_i(t) = \begin{cases} 1 & \text{if } \phi(X_i(t)) < E_i \\ 0 & \text{if } \phi(X_i(t)) \geq E_i \end{cases}, \tag{S18}$$

where $\phi(\cdot)$ is the standard normal cumulative distribution function. Hence, $\phi(X_i(t)) \in (0,1)$. Moreover, $\phi(X_i(t))$ has a uniform distribution (indeed, all continuous random variables are uniformly distributed when transformed with their distribution function, a fact that can be found in most graduate textbooks in probability; e.g., Theorem 2.1.10 in Casella and Berger 2001). Figure S1 illustrates how a random sample from a normal distribution (red points), once transformed through its distribution function (solid line), yields a random sample from a uniform distribution (purple points).

Because $\phi(X_i(t)) \sim \text{Uniform}(0,1)$, $P(\phi(X_i(t)) < E_i) = E_i$, and $P(\phi(X_i(t)) \geq E_i) = 1 - E_i$. Hence, $P(Y_i(t) = 1) = E_i$ and $P(Y_i(t) = 0) = 1 - E_i$, meaning $Y_i(t) \sim \text{Bernoulli}(E_i)$. In our simulations, we sample $\mathbf{X}(t)$ to calculate $\mathbf{Y}(t)$ according to equation (S18), and then use $\mathbf{Y}(t)$ to determine which local populations go from occupied to unoccupied from time step t to time step $t + \Delta t$.

Importantly, the correlation structure embedded in the multivariate distribution $\mathbf{X}(t)$ is likewise embedded in the multivariate distribution of extinction events, $\mathbf{Y}(t) = (Y_1(t), Y_2(t), \ldots, Y_n(t))$, because $Y_i(t)$ is a monotonic function of $X_i(t)$.

Figure S2 shows a version of this model for 2 patches where the correlation is very strong in the environmental variables (Fig. S2a) such that, when the latent variables are transformed

Supplemental Material (not copyedited or formatted) for: Nicholas Kortessis, Gregory Glass, Andrew Gonzalez, Nick W. Ruktanonchai, Margaret W. Simon, Burton Singer, Robert D. Holt. 2025. "Metapopulations, the Inflationary Effect, and Consequences for Public Health."
The American Naturalist 205(3). DOI: https://doi.org/10.1086/733896.

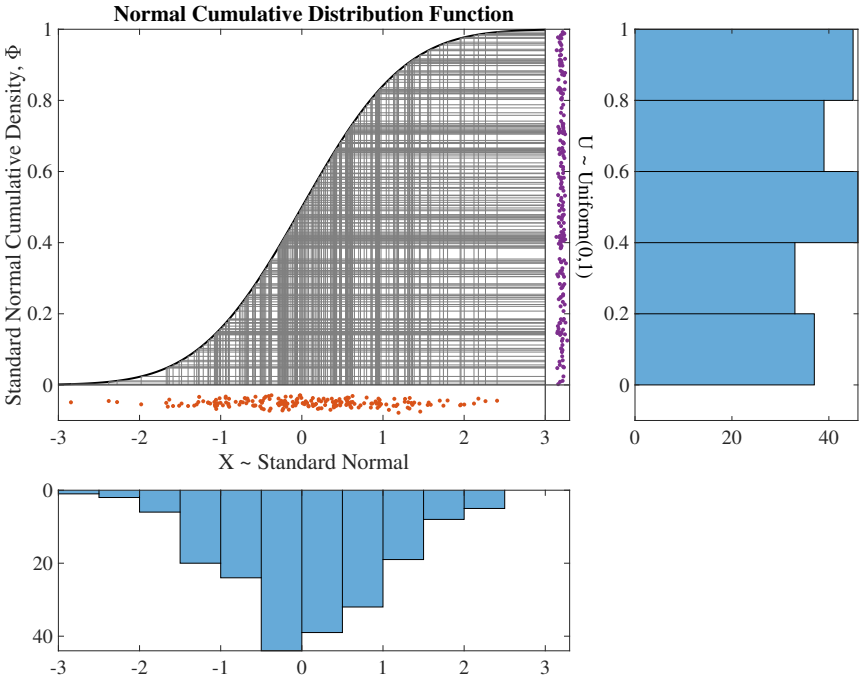

Figure S1: Demonstration of the fact that a sample from a standard normal distribution (red points in main figure; frequency distribution shown in the lower panel) can be transformed to a random sample from a uniform distribution (purple points; frequency distribution shown in the right panel). The transformation is done by the normal cumulative distribution function, which is the curve in the main panel. Gray lines show the mapping of a random sample from the standard normal through the distribution function to yield a value between 0 and 1.

to extinction events (Fig. S2b), the spatio-temporal pattern of extinction events shows strong synchrony over space (Fig. S2c).

S2.1 Simulation details

To simulate extinction times and mean occupancy with this model, we chose a population with $n = 50$ patches, and we set $\Delta t = 0.005$. Each occupied patch has extinction probability, $E_i(t) = 1 - \exp(-e\Delta t)$, with $e = 0.25$, meaning that the expected time to extinction is 4 units of time. We also chose $c = 0.5$ such that colonization probability of any unoccupied patch in a small time step is $C_i(t) = 1 - \exp(-cP(t)\Delta t)$. Under this model, when $P(t) = 0.5$, patches have an expected time being unoccupied of ≈ 4 units of time. At this point, extinction and colonizations equal each other in the large patch number limit, meaning $P(t) = 0.5$ is the equilibrium occupancy for

Supplemental Material (not copyedited or formatted) for: Nicholas Kortessis, Gregory Glass, Andrew Gonzalez, Nick W. Ruktanonchai, Margaret W. Simon, Burton Singer, Robert D. Holt. 2025. "Metapopulations, the Inflationary Effect, and Consequences for Public Health."
The American Naturalist 205(3). DOI: https://doi.org/10.1086/733896.

the deterministic form of the model.

For each simulation, we begin with 13 of the 25 patches initially occupied, i.e., $O_i(t=0)=1$ for $i=1,2,\ldots,13$ and $O_j(t=0)=0$ for all $j\neq i$. Each time step, we randomly sample $\mathbf{X}(t)$ and calculate $\mathbf{Y}(t)$ for each patch. If a patch is occupied and $Y_i(t)=1$, then the patch becomes unoccupied in the next time step. For unoccupied patches in time t, we take a random sample from a Binomial random variable with $n(1-P(t))$ trials (i.e., the number of unoccupied patches) and "success" probability $C(t)$. Sampling from a Binomial distribution implies independence of colonization events across unoccupied patches, a simplifying assumption made here for simplicity. Non-independence of extinction is sufficient to demonstrate the effect of spatio-temporal heterogeneity.

We sampled this process for every time increment over 100 units of time for a total of 20,000 increments (i.e., $100/\Delta t = 20{,}000$ time steps) and evaluated whether the metapopulation had gone extinct (i.e., $P(t)=0$). If it had, we recorded the first time of metapopulation extinction. If it had not yet gone extinct, we continued for another 100 units of time, repeating this process until the metapopulation had gone extinct.

We repeated this process for 100 replicate sample paths of extinction and colonization events for a single value of ρ_E. Extinction times are approximately log-normally distributed across the replicate simulations, so we plotted extinction times on the $\log_{10}$ scale.

S3 Inflated abundance in a source-sink model with spatio-temporal heterogeneity

Here we provide analytical justification for the inflationary effect in a model with a fluctuating sink with constant immigration.

Let $N(t)$ be the density of individuals in the sink at time t ($t=0,1,2,\ldots$) and $r(t)$ be a random variable describing the per-capita growth rate in the sink patch in the absence of any immigration. We assume that $r(t)$ is i.i.d. over time and that $E[r(t)]=\bar{r}<0$, such that the population declines exponentially in the sink with long-term growth rate $\bar{r}<0$. As conditions in the sink fluctuate stochastically, but are on average negative, the patch is better described as a *stochastic sink*. Finally, we assume that there is a constant source of immigrants that enter the sink. The number that enter in a given time interval per area of the sink is I.

The population size in time $t+1$ is then given by the following equation:

$$N(t+1)=N(t)e^{r(t)}+I. \tag{S19}$$

The per-capita growth rate for this model is

$$g(r,N)\equiv \ln N(t+1)-\ln N(t)=\ln\{e^{r(t)}+I/N(t)\}. \tag{S20}$$

Supplemental Material (not copyedited or formatted) for: Nicholas Kortessis, Gregory Glass, Andrew Gonzalez, Nick W. Ruktanonchai, Margaret W. Simon, Burton Singer, Robert D. Holt. 2025. "Metapopulations, the Inflationary Effect, and Consequences for Public Health."
The American Naturalist 205(3). DOI: https://doi.org/10.1086/733896.

This equation allows one to make some observations about the qualitative nature of the dynamics in the model. The first observations is that the population is bounded from above because

$$\lim_{N\to\infty} g(r,N) \to r(t) \tag{S21}$$

which, on average, is negative because $r(t)$ is negative on average. Thus, the population has a tendency to decline when its density is too high. (Note that this analysis requires the technical assumption that $r(t)$ is bounded from above by a finite value, a technical assumption that does not restrict the generality of the result.)

Moreover, we know that population size is bounded from below because

$$\lim_{N\to 0} g(r,N) \to \infty, \tag{S22}$$

and as such, the population has a strong tendency to recover as it becomes rare. This is the strong stabilizing effect of immigration.

Taken together, these two observations suggest that the population stays within some range of population sizes and does not increase to infinity, nor decline to zero. Hence, at some temporal scale, the average per-capita growth rate is 0, i.e., $E[g(r,N)] = 0$.

This equilibrium is straightforward to define in the case of a constant environment, i.e., $r(t) = \bar{r}$ for all t. Equilibrium population size, N^*, satisfies the equation

$$g(\bar{r},N^*) = 0 \Rightarrow e^{\bar{r}} + I/N^* = 1. \tag{S23}$$

The solution to (S23) is $N^* = I/(1-e^{\bar{r}})$, which is the equilibrium population size in a constant environment.

By nature of the fact the population is bounded from below and bounded from above by the arguments above (provided $E[r(t)] < 0$), then it follows that, in the long-term, the population neither grows nor declines, on average. Hence, the long-term growth rate of the population is $E[g(r(t),N(t))] = 0$. A small-variance approximation of g around the constant environment case (i.e., $r^* = \bar{r}$ and $N^* = I/(1-e^{\bar{r}})$), yields the following equation for the growth rate at time t:

$$\begin{aligned} g(r,N) = g(\bar{r},N^*) + e^{\bar{r}}(r-\bar{r}) - \frac{(1-e^{\bar{r}})^2}{I}(N-N^*) + \frac{1}{2}\frac{e^{\bar{r}}}{1-e^{\bar{r}}}(r-\bar{r})^2 \\ + \frac{1}{2}\frac{(1+e^{\bar{r}})(1-e^{\bar{r}})^3}{I^2}(N-N^*)^2 + o(\sigma^2), \end{aligned} \tag{S24}$$

where we assume that $r-\bar{r} = O(\sigma)$ and $N-N^* = O(\sigma)$, σ small.

Noting that $g(\bar{r},N^*) = 0$, and taking the expectations of the left and right hand sides of (S24) yields

$$E[g(r,N)] = -\frac{(1-e^{\bar{r}})^2}{I}E[(N-N^*)] + \frac{1}{2}\frac{e^{\bar{r}}}{1-e^{\bar{r}}}\mathrm{Var}(r) + \frac{1}{2}\frac{(1+e^{\bar{r}})(1-e^{\bar{r}})^3}{I^2}\mathrm{Var}(N) + o(\sigma^2). \tag{S25}$$

Supplemental Material (not copyedited or formatted) for: Nicholas Kortessis, Gregory Glass, Andrew Gonzalez, Nick W. Ruktanonchai, Margaret W. Simon, Burton Singer, Robert D. Holt. 2025. "Metapopulations, the Inflationary Effect, and Consequences for Public Health." The American Naturalist 205(3). DOI: https://doi.org/10.1086/733896.

Since $E[g(r,N)] = 0$, simple rearrangement of (S25) yield the following approximate difference between the average population size and the equilibrium population size under constant conditions:

$$E[N] - N^* \approx \frac{1}{2}\left[\frac{Ie^{\bar{r}}}{(1-e^{\bar{r}})^3}\mathrm{Var}(r) + \frac{(1+e^{\bar{r}})(1-e^{\bar{r}})}{I}\mathrm{Var}(N)\right] \geq 0, \tag{S26}$$

where the approximation sign denotes $o(\sigma^2)$, and the inequality follows from the fact that all the terms on the right hand side of the approximation are non-negative provided $\bar{r} < 0$. Hence, $E[N] \geq N^*$, meaning that the average population size under variable local growth rates is larger than the model under constant growth rates. This is simple example of the inflationary effect for small variation in local growth rates.

S3.1 Quantifying the magnitude of spatio-temporal heterogeneity

The source-sink model has spatio-temporal heterogeneity because the sink's growth rates fluctuate while it is implied that the source's growth rates do not. Constant immigration to the source is most consistent with a constant fraction of the population in the source that leaves each time step. This also requires that the population size in the source be at an equilibrium

By making the dynamics of the source patch explicit, we can quantify the spatio-temporal variability σ^2_{ST}.

Label the source as patch 1 and the sink as patch 2. Assume that the source has density-independent growth rate r_1, a constant, that is reduced by density-dependence with per-capita strength α. Following growth, a fraction d of individuals disperse to the sink. With these assumptions, the dynamics in the source follow

$$N_1(t+1) = N_1(t)e^{r_1 - \alpha N_1(t)}(1-d), \tag{S27}$$

and the total number of dispersers to the sink in one unit of time is $I(t) = N_1(t)\exp(r_1 - \alpha N_1(t))d$. Immigration becomes constant when the source population reaches equilibrium, N_1^*, can be found by solving

$$N_1^* = N_1^* e^{r_1 - \alpha N_1^*}(1-d), \tag{S28}$$

and has the non-trivial solution

$$N_1^* = \frac{r_1 + \ln\{1-d\}}{\alpha}. \tag{S29}$$

Note that because $0 \leq d \leq 1$, $\ln\{1-d\} \leq 0$, meaning that $r_1 > \ln\{1-d\}$ in order for the source population to have a positive equilibrium density.

At this equilibrium, the growth rate prior to dispersal in the source is $\exp(r_1 - \alpha N_1^*) = 1/(1-d) \geq 0$, which is a constant. The number of immigrants to the sink at equilibrium can also be calculated as

$$I = d\exp(r - \alpha N_1^*)N_1^* = \frac{d}{1-d} \cdot \frac{r_1 + \ln(1-d)}{\alpha} \tag{S30}$$

Supplemental Material (not copyedited or formatted) for: Nicholas Kortessis, Gregory Glass, Andrew Gonzalez, Nick W. Ruktanonchai, Margaret W. Simon, Burton Singer, Robert D. Holt. 2025. "Metapopulations, the Inflationary Effect, and Consequences for Public Health."
The American Naturalist 205(3). DOI: https://doi.org/10.1086/733896.

With the growth rates in hand, we can define the fitness factor as the local growth rates themselves, which are

$$\begin{aligned} F(t,1) &= -\ln(1-d) \\ F(t,2) &= r(t). \end{aligned} \tag{S31}$$

Given that the growth rate in the source patch is constant, the temporal mean is $E_t[F|x=1] = -\ln(1-d)$ and so the temporal variance is $\mathrm{Var}_t[F|x=1] = 0$. The temporal variance is zero in this model regardless of emigration and immigration rates. The temporal mean and variance for the sink growth rates are $E_t[F|x=2] = \bar{r}$ and $\mathrm{Var}(F|x=2) = \sigma_r^2$. Since both patch types are equally common (i.e., there is one of each), we weight their contribution to growth equally in the spatial variance, which is

$$\begin{aligned} \sigma_S^2 &= \mathrm{Var}_x(E_t[r|x]) \\ &= \frac{(-\ln(1-d)-\bar{r})^2}{4}. \end{aligned} \tag{S32}$$

The temporal variance is calculated as

$$\begin{aligned} \sigma_T^2 &= \mathrm{Var}_t(E_x[r|t]) \\ &= \mathrm{Var}_t\left(\frac{-\ln(1-d)+r(t)}{2}\right) \\ &= \mathrm{Var}_t\left(\frac{r(t)}{2}\right) \\ &= \frac{\sigma_r^2}{4}. \end{aligned} \tag{S33}$$

Finally, the spatio-temporal variance is

$$\begin{aligned} \sigma_{ST}^2 &= E_x[\mathrm{Var}_t(r|x)] - \sigma_T^2 \\ &= \frac{1}{2}\Big(\mathrm{Var}_t(r|x=1) + \mathrm{Var}_t(r|x=2)\Big) - \sigma_T^2 \\ &= \frac{1}{2}(0+\sigma_r^2) - \sigma_T^2 \\ &= \frac{\sigma_r^2}{2} - \frac{\sigma_r^2}{4} \\ &= \frac{\sigma_r^2}{4}. \end{aligned} \tag{S34}$$

On a relative scale, the contribution of spatio-temporal variance to total variance on the landscape can be written as

$$\frac{\sigma_{ST}^2}{\sigma_T^2+\sigma_S^2+\sigma_{ST}^2} = \frac{1}{2+(-\ln(1-d)-\bar{r})^2/\sigma_r^2}. \tag{S35}$$

This shows that the absolute measure of spatio-temporal variance depends on the variance in sink growth rates, σ_r^2, whereas the contribution to the total variance on the landscape also relies on dispersal from the source, d, as well as the temporal average growth rate in the sink, $\bar{r}$.

Supplemental Material (not copyedited or formatted) for: Nicholas Kortessis, Gregory Glass, Andrew Gonzalez, Nick W. Ruktanonchai, Margaret W. Simon, Burton Singer, Robert D. Holt. 2025. "Metapopulations, the Inflationary Effect, and Consequences for Public Health."
The American Naturalist 205(3). DOI: https://doi.org/10.1086/733896.

	Variance Component		
	σ_T^2	σ_S^2	σ_{ST}^2
Expression	$\sigma_r^2/4$	$(-\ln(1-d)-\bar{r})^2/4$	$\sigma_r^2/4$

Table S1: Components of the variance in growth rates in the source sink model. $\sigma_r^2 = \text{Var}(r(t))$ is the variance of the growth rates in the sink, and d is the fraction of individuals that disperse from the source to the sink in a unit of time.

S4 Derivation of the measure of the inflationary effect

To derive the measure of the inflationary effect, we need the growth rate of model (3) provided in the main text at the scale of the metapopulation. At the scale of the metapopulation, we can define $\bar{N} = \frac{1}{n}\sum_{i=1}^{n} N_i$ as the metapopulation density (assuming all patches are the same size). This density represents the dynamics across all space on average. The growth rate at the metapopulation scale is then

$$\frac{d\bar{N}}{dt} = \frac{1}{n}\sum_{i=1}^{n}\frac{dN_i}{dt}, \tag{S36}$$

and so is the average of the local patch growth rates. Thus, the per-capita growth rate at the metapopulation scale is

$$\frac{1}{\bar{N}}\frac{d\bar{N}}{dt} = \frac{1}{n}\sum_{i=1}^{n}\frac{1}{\bar{N}}\frac{dN_i}{dt}. \tag{S37}$$

Plugging in the expression for the patch-specific growth rates (eqn 3) of the main text into (S37) yields

$$\frac{1}{\bar{N}}\frac{d\bar{N}}{dt} = \frac{1}{n}\sum_{i=1}^{n} r_i(t)\nu_i(t) + \frac{1}{n}\sum_{i=1}^{n}\sum_{j\neq i} m_{ij}\nu_j(t) - \frac{1}{n}\sum_{i=1}^{n} m_i\nu_i(t), \tag{S38}$$

where $\nu_i(t) = N_i(t)/\bar{N}$ is the *relative density in patch i at time t*. The second summation on the right hand side of (S38) is the average rate of immigration across all n patches (in per-capita terms). The third summation is the average rate of emigration across all n patches (again, in per-capita terms). As no individuals die during dispersal in the model, the total rates of emigration and immigration are the same, i.e.,

$$\frac{1}{n}\sum_{i=1}^{n}\sum_{j\neq i} m_{ij}\nu_j(t) = \frac{1}{n}\sum_{i=1}^{n}\sum_{j\neq i} m_{ji}\nu_i(t) = \frac{1}{n}\sum_{i=1}^{n} m_i\nu_i(t). \tag{S39}$$

Using (S39) in (S38) yields the following expression for the per-capita growth rate at the regional scale:

$$\frac{1}{\bar{N}}\frac{d\bar{N}}{dt} = \frac{1}{n}\sum_{i=1}^{n} r_i(t)\nu_i(t) = \bar{r}(t) + \text{cov}_i(r_i(t),\nu_i(t)), \tag{S40}$$

where $\bar{r}(t) = (1/n)\sum_{i=1}^{n} r_i(t)$ is the spatial average growth rate at time t, and the last equality follows because the average of a product is the product of the averages plus a covariance between

Supplemental Material (not copyedited or formatted) for: Nicholas Kortessis, Gregory Glass, Andrew Gonzalez, Nick W. Ruktanonchai, Margaret W. Simon, Burton Singer, Robert D. Holt. 2025. "Metapopulations, the Inflationary Effect, and Consequences for Public Health."
The American Naturalist 205(3). DOI: https://doi.org/10.1086/733896.

the two (the average of $\nu_i(t)$ is $\bar{\nu}(t) = 1$). Note that the covariance here is defined for a finite set of patches, rather than the typical interpretation in probability as a covariance over a probability measure. However, its properties should generally be identical (within sampling error) to the probabilistic interpretation when the finite set of locations under question is a random sample of space.

The metapopulation scale growth rate applies at a single point in time. The long-term growth rate in this environment is the average across the set of environmental conditions that are experienced (including their possible temporal structure). We use the expectation operator from probability theory to represent the -average across these possible conditions (and their associated probabilities of occurrence). Given some time t far into the future, the long-term average metapopulation growth rate is

$$E_t\left[\frac{1}{\bar{N}}\frac{d\bar{N}}{dt}\right] = E_t[\bar{r}(t)] + E_t\left[\text{cov}_i\Big(r_i(t), \nu_i(t)\Big)\right], \tag{S41}$$

which gives the appropriate per-capita measure of population growth in models with continuously variable population densities in spatially and temporally varying environments.

Note that in stochastic representations of the environment in continuous-time models typically involves stochastic differential equations, the calculus of which is not straightforward. A choice must be made in the calculus of the integral to evaluate the average. Itô and Stratonovich calculuses are two methods by which to evaluate long-term growth rates in such models, with the long-term patch growth rate under Itô calculus differing from the average of the distribution of $r_i(t)$ (see Schreiber et al. (2023) for an example). However, such differences in calculus of growth rates has no impact on the quantification of the inflationary effect as the effect cancel each other out, as can be seen below.

When applied to the per-capita growth rate, the inflationary effect is the amount to which the growth rate is enhanced in reference to a hypothetical scenario without spatiotemporal variability. Originally, Gonzalez and Holt (2002) constructed a reference scenario in which there is no temporal variation. We follow that definition here and represent a model wherein the environment is constant, but retains the effects of temporal variability.

Temporal variability in a continuous-time model in a single patch i without dispersal (i.e., all $m_{ij} = 0$) is described by the time average per-capita growth rate,

$$\tilde{r}_i \equiv E_t\left[\frac{1}{N_i}\frac{dN_i}{dt}\right], \tag{S42}$$

which we write as $\tilde{r}_i$, indicating the time average in patch i.

Applying each patch's time-average growth rate in the model with dispersal yields a system of linear ordinary differential equations as

$$\frac{d\mathbf{N}}{dt} = \mathbf{A}\mathbf{N}, \tag{S43}$$

Supplemental Material (not copyedited or formatted) for: Nicholas Kortessis, Gregory Glass, Andrew Gonzalez, Nick W. Ruktanonchai, Margaret W. Simon, Burton Singer, Robert D. Holt. 2025. "Metapopulations, the Inflationary Effect, and Consequences for Public Health."
The American Naturalist 205(3). DOI: https://doi.org/10.1086/733896.

where $\mathbf{N} = (N_1, N_2, \ldots, N_n)^T$ is a column vector of local population densities, and $\mathbf{A} = (A_{ij})$ gives the rates of change in patch i contributed by patch j. The diagonal elements, $a_{ii} = \tilde{r}_i - m_i$, describe the emigration discounted growth rate of a patch, and the off-diagonal elements, $a_{ij} = m_{ij}$ describe movement rates between patches. This model is a linear model that grows exponentially at the rate given by the dominant eigenvalue of $\mathbf{A}$ and has a stable spatial distribution given by the right eigenvector of $\mathbf{A}$.

The stable spatial distribution can be rescaled to relative density, which we label with a tilde as $\tilde{v}_i$ to indicate that the relative density applies to the stable distribution defined by constant growth rates $\tilde{r}_i$.

The dominant eigenvalue of $\mathbf{A}$, which is the metapopulation scale per-capita growth rate, can be written as

$$\frac{1}{\bar{N}}\frac{d\bar{N}}{dt} = \frac{1}{n}\sum_{i=1}^{n}\tilde{r}_i\tilde{v}_i = \frac{1}{n}\sum_{i=1}^{n}\tilde{r}_i + \mathrm{cov}_i\left(\tilde{r}_i, \tilde{v}_i\right). \tag{S44}$$

In (S44), the covariance is a constant, rather than a time-varying function.

The inflationary effect is simply how much the growth rate in the actual model deviates from the reference model. Given that the reference model has pure spatial variation and pure temporal variation, any differences can be attributable to spatiotemporal variation. Subtracting (S44) from (S41) gives an experession for the inflationary effect, which is

$$\begin{aligned}\text{Inflationary Effect} &= E_t[\bar{r}(t)] - \frac{1}{n}\sum_{i=1}^{n}\tilde{r}_i + E_t\left[\mathrm{cov}_i\Big(r_i(t), v_i(t)\Big)\right] - \mathrm{cov}_i\left(\tilde{r}_i, \tilde{v}_i\right)\\ &= E_t\left[\mathrm{cov}_i\Big(r_i(t), v_i(t)\Big)\right] - \mathrm{cov}_i\Big(\tilde{r}_i, \tilde{v}_i\Big),\end{aligned} \tag{S45}$$

where the final line follows because

$$E_t[\bar{r}(t)] = E_t\left[\frac{1}{n}\sum_{i=1}^{n}r_i(t)\right] = \frac{1}{n}\sum_{i=1}^{n}E_t[r_i(t)] = \frac{1}{n}\sum_{i=1}^{n}\tilde{r}_i, \tag{S46}$$

and so the first two terms in the first line cancel out. The last line of equation (S45) is equation (4) of the main text.

S4.1 On the rate of dispersal necessary for the inflationary effect

We stipulated that dispersal was required for the inflationary effect so long as it is not "too much" dispersal. What constitutes "too much"? A clear case of too much comes from the metapopulation model given by equation (3) of the main text in the limit as $m \to \infty$. In this case, the metapopulation converges on a "well-mixed" spatial distribution in which individuals have an equal probability of being present in any patch on the landscape. As such, the relative density is the same in every patch (i.e., $v_i = 1$ for all patches). Without any variation in relative

Supplemental Material (not copyedited or formatted) for: Nicholas Kortessis, Gregory Glass, Andrew Gonzalez, Nick W. Ruktanonchai, Margaret W. Simon, Burton Singer, Robert D. Holt. 2025. "Metapopulations, the Inflationary Effect, and Consequences for Public Health."
The American Naturalist 205(3). DOI: https://doi.org/10.1086/733896.

density, the covariance between local fitness and density is zero and so there is no inflationary effect. Clearly "well-mixed" is too much dispersal.

The more general statement about "too much" dispersal comes from studies of the inflationary effect using models of the general form of eqn (3). Those studies typically find a hump-shaped relationship between the landscape level growth (or abundance) and the dispersal rate m (e.g., Fig. 4 of Roy et al. 2005). The front half of the hump comes from the fact that some dispersal moves individuals to patches in the landscape that are currently declining but will soon be expanding. This increased movement, on average, concentrates individuals in favorable patches on the landscape. The latter half of the hump comes from the fact that more movement begins to move individuals out of these favorable locations. Hence, the determination of "too much" depends on the temporal structure of the environment. If the temporal autocorrelation of the environment is short, comparatively high emigration rates may still not be "too much" because environments change quickly and only highly dispersive individuals will be able to keep up with continuously moving favorable locations. If the temporal autocorrelation is long, then comparatively slow emigration rates may nonetheless constitute "too much" dispersal as local patch conditions tend to stay favorable for longer.

The hump-shaped relationship between the metapopulation growth rate and the rate of movement, however, does not necessarily indicate a negative inflationary effect. The types of dispersal and environmental structure considered has been limited such that (at least to our knowledge) there are no demonstrated deflationary effects. For all dispersal rates greater than zero, prior models have shown positive inflationary effects, but the hump-shape indicates that the magnitude of the inflationary effect varies non-monotonically with dispersal. For sufficiently high movement rates, the inflationary effect, while positive, will be so small as to be immeasurable in any real system.

S5 Details of the model of disease transmission

To illustrate the effects of spatio-temporal heterogeneity on the spread of infectious disease, we use the following two-patch SIR model:

$$\begin{aligned}
\frac{dS_i}{dt} &= -\beta_i(t)\frac{S_i I_i}{N_i} - mS_i + mS_j \\
\frac{dI_i}{dt} &= \beta_i(t)\frac{S_i I_i}{N_i} - \gamma I_i - mI_i + mI_j \quad (i = 1, 2) \\
\frac{dR_i}{dt} &= \gamma I_i,
\end{aligned} \tag{S47}$$

where S_i, I_i, and R_i are the number of susceptible, infectious, and recovered individuals in patch i, respectively, $\beta_i(t)$ is the time and location-specific transmission rate, m is the movement rate, and γ is the rate of recovery from infection. In this simple form of the of model, we assume that individuals may only be in one of these three classes such that $N_i(t) = S_i(t) + I_i(t) + R_i(t)$.

Supplemental Material (not copyedited or formatted) for: Nicholas Kortessis, Gregory Glass, Andrew Gonzalez, Nick W. Ruktanonchai, Margaret W. Simon, Burton Singer, Robert D. Holt. 2025. "Metapopulations, the Inflationary Effect, and Consequences for Public Health."
The American Naturalist 205(3). DOI: https://doi.org/10.1086/733896.

As a simple illustration of asynchrony, we consider a scenario where the transmission rate oscillates between two values periodically according to the following equations (and shown in Figure S3):

$$\beta_1(t) = \begin{cases} \beta_0 & \text{for } 2nT < t < (2n+1)T \\ \beta_0(1-\epsilon) & \text{otherwise} \end{cases}, \qquad \beta_2(t) = \begin{cases} \beta_0 & \text{for } 2nT - \tau < t < (2n+1)T - \tau \\ \beta_0(1-\epsilon) & \text{otherwise} \end{cases}, \tag{S48}$$

where $n = \{0, 1, 2, 3, \ldots\}$ is the set of natural numbers (zero inclusive), and ϵ is the proportional reduction in transmission from non-pharmaceutical interventions ($0 \leq \epsilon \leq 1$). As such, it is the effectiveness of any non-pharmaceutical intervention (hereafter NPI).

The parameter τ is the time-shift between the change in state of the two patches. Patch two begins NPIs τ units of time prior to patch 1 and releases them τ units prior to patch 1 as well. Time shifts can be anywhere from 0, when the two patches are completely in sync, to T, when the patches are completely out of sync (note that because the square wave function is periodic, τ can take any real value, each of which has a mapping to the space $\tau \in [0, T]$).

The time shift is related to Ω, the NPI overlap, with the following relationship

$$\Omega = 1 - \frac{\tau}{T}, \tag{S49}$$

where τ/T is the fraction of a half period where the patches are in different states. Each of the half periods are the same duration, so it is also the fraction of the entire period that the two patches are in different states. Therefore, $1 - \tau/T$ is the fraction of time the two patches are in the same state, i.e., the amount of overlap.

S5.1 Spatio-temporal variance

The fitness factor for this model is β, which changes over space and time. To calculate the three components of variability in β, we need the conditional spatial and temporal means and variances.

The temporal means and variances are based on the two values of the square-wave function, β_0 and $\beta_0(1-\epsilon)$, which are equally common on a cycle. Since they are equally common in both patches, the temporal average β in patch x is $E_t[\beta_x] = \beta_0(1 - \epsilon/2)$.

The pure spatial variance is the variance among patches in the temporal average transmission rate. The temporal average transmission rates are identical in the two patches, meaning there is no spatial variability. Hence,

$$\sigma_S^2 = \mathrm{Var}_x(E_t[\beta]) = 0. \tag{S50}$$

The pure temporal variance is the variance over times in the average spatial transmission rate. To determine this, we partition time within a cycle into four periods, described below and

Supplemental Material (not copyedited or formatted) for: Nicholas Kortessis, Gregory Glass, Andrew Gonzalez, Nick W. Ruktanonchai, Margaret W. Simon, Burton Singer, Robert D. Holt. 2025. "Metapopulations, the Inflationary Effect, and Consequences for Public Health." The American Naturalist 205(3). DOI: https://doi.org/10.1086/733896.

demonstrated in Figure S3. The first time period, t_1, is the time when both patches have the fast transmission rate, i.e. $\beta_1 = \beta_2 = \beta_0$. The third time period, t_3, is the time when both patches have the slow transmission rate $\beta_1 = \beta_2 = \beta_0(1-\epsilon)$. Time periods two, t_2, and four, t_4, are those where the patches are in different states; one has transmission rate β_0 and the other has transmission rate $\beta_0(1-\epsilon)$ and the two time periods are distinguished by the identities of the patches in the different states.

Time periods one and three together comprise Ω fraction of time, and time periods two and four together comprise $1-\Omega$ fraction of time.

The average growth rate over space at any time, $E_x[\beta(x,t)|t]$ can be found by using this time partition. The average across the two patches in each time period are

$$\begin{aligned} E_x[\beta(x,t)|t \in t_1] &= \beta_0 \\ E_x[\beta(x,t)|t \in t_2] &= \beta_0\left(1-\frac{\epsilon}{2}\right) \\ E_x[\beta(x,t)|t \in t_3] &= \beta_0(1-\epsilon) \\ E_x[\beta(x,t)|t \in t_4] &= \beta_0\left(1-\frac{\epsilon}{2}\right). \end{aligned} \tag{S51}$$

The average of these spatial averages across time is

$$E_t[E_x[\beta(x,t)]] = \beta_0\left(1-\frac{\epsilon}{2}\right). \tag{S52}$$

And so the temporal variance of these spatial averages is

$$\sigma_T^2 = \mathrm{Var}_t(E_x[\beta(x,t)|t]) = \Omega\left(\frac{\beta_0\epsilon}{2}\right)^2. \tag{S53}$$

The spatio-temporal variance can be written as

$$\sigma_{ST}^2 = E_x[\mathrm{Var}_t(\beta|x)] - \mathrm{Var}_t(E_x[\beta|t]). \tag{S54}$$

To calculate this quantity, we need the spatial average of the conditional variance over time, $E_x[\mathrm{Var}_t(\beta|x)]$, as the second term on the right-hand side of the expression is the pure temporal variance.

The temporal variance in a given patch x can be found by noting that the two values in a period, which are each equally common in time, deviate from the temporal average by $\pm\beta_0\epsilon/2$. Hence, the variance over time is

$$\mathrm{Var}_t(\beta|x) = \frac{1}{2}\left(\frac{\beta_0\epsilon}{2}\right)^2 + \frac{1}{2}\left(-\frac{\beta_0\epsilon}{2}\right)^2 = \left(\frac{\beta_0\epsilon}{2}\right)^2. \tag{S55}$$

This variance is the same for both patches so that

$$E_x[\mathrm{Var}_t(\beta|x)] = \left(\frac{\beta_0\epsilon}{2}\right)^2. \tag{S56}$$

Supplemental Material (not copyedited or formatted) for: Nicholas Kortessis, Gregory Glass, Andrew Gonzalez, Nick W. Ruktanonchai, Margaret W. Simon, Burton Singer, Robert D. Holt. 2025. "Metapopulations, the Inflationary Effect, and Consequences for Public Health."
The American Naturalist 205(3). DOI: https://doi.org/10.1086/733896.

Using (S56) and (S53) in (S54) yields

$$\sigma^2_{ST} = (1-\Omega)\left(\frac{\beta_0\epsilon}{2}\right)^2. \tag{S57}$$

Putting this on a scale of the spati-temporal variations contribution to the total variation in the transmission rate yields

$$\frac{\sigma^2_{ST}}{\sigma^2_S+\sigma^2_T+\sigma^2_{ST}} = \frac{(1-\Omega)\left(\frac{\beta_0\epsilon}{2}\right)^2}{0+\Omega\left(\frac{\beta_0\epsilon}{2}\right)^2+(1-\Omega)\left(\frac{\beta_0\epsilon}{2}\right)^2} = 1-\Omega, \tag{S58}$$

which shows that all the variation is temporal-only when NPIs are exactly in sync and all the variation is spatio-temporal when NPIs are exactly out of sync.

S5.2 Calculating the long-term growth rate

We find the long-term metapopulation growth rate of an invading pathogen in Figure 5a by assuming that the fraction in the population in the infectious class is very small, which is suitable for much of the early dynamics of COVID-19 because the disease was distributed worldwide, but had infected a very small percentage of the population in any given locality of moderate spatial scale. We do this by simulating (S47) while rescaling the density of the infectious class to keep it arbitrarily small. We run this simulation over multiple cycles of $\beta_i(t)$ until a stationary distribution for $\nu_i = I_i/\bar{I}$ is reached. At that point, we simulate the dynamics of I_i for more cycle and measure the long-term metapopulation rate of spread as

$$\frac{\Big(I_1(2T)+I_2(2T)\Big)-\Big(I_1(0)+I_2(0)\Big)}{2T}, \tag{S59}$$

which is the average rate of change of the infectious class at the metapopulation scale. This allows us to isolate the average effect of spatio-temporal heterogeneity when a pathogen is introduced into a population and is sufficiently uncommon so as not to experience self-regulation by limited susceptible hosts.

Figures S4 and S5 show the effects of increasing the effectiveness of NPIs and the duration of NPIs on the long-term growth rate under different overlap levels and movement scenarios.

Stochastic model

We included stochastic variation in transmission rates in addition to deterministic variation from NPIs. To do so, we used a discrete-time version of the above continuous-time SIR model where time steps correspond to days. To model stochasticity in the transmission rate, we assumed $\beta_i(t)$ in any time point follows a truncated normal distribution. The mean of the normal distribution

at time t is given by the deterministic component of the model from eqn (S48), and the variance of the normal distribution is assumed to be σ^2. The truncated normal is used to ensure that the transmission rate is not a negative value.

For the stochastic model, we chose infectious duration $1/\gamma = 4.5$ days in both patches and a baseline transmission rate of $\beta_0 = 0.375$ d^{-1}. This corresponds to a daily growth rate of 1.53 d^{-1}, case doubling times of approximately 4.5 days, and R_0 value about 1.7 (in a completely susceptible population). We illustrate the inflationary effect with a highly effective NPI regime (95% reduction in baseline transmission) that cycles every 60 days (30 days NPI regime and 30 days "business as usual"). We chose chose $\sigma = 0.1$ to represent stochastic variation in transmission in addition to NPIs.

To illustrate how the inflationary effect arises from positive fitness-densities covariances, on average, over time, we kept track of relative density of infectious individuals in each patch and the fitness at each time step. Relative density of infectious individuals in patch i at time t was calculated as $I_i(t)/\bar{I}(t)$ where $\bar{I}(t) = (I_1(t) + I_2(t))/2$ is the average infectious density. Fitness for the discrete-time model was calculated as $\lambda_i(t) = \exp(\beta_i(t) - \gamma)$, which is analogous to the continuous-time per-capita growth rate ($1/I \cdot dI/dt$) when the time scale is very short.

At each time step, we calculated the covariance across the two patches between relative infectious density and local fitness. We plotted the dynamics of this spatial covariance for each of the two Ω values considered in Figure 5 of the main text. The dynamics are shown by the solid lines in Figure S5.2. The average over time of these covariance gives the inflationary effect because $\text{cov}(\tilde{v}, \tilde{r}) = 0$ by the fact that the temporal average growth rate is the same in both patches. The average fitness-density covariance is given by the dotted lines in Figure S5.2, showing that the fitness-density covariance is positive on average with asynchrony and zero on average when completely synchronized.

References

Casella, G. and R.J. Berger. 2001. *Statistical Inference*. Cengage Learning.

Ghosh, S, L.W. Sheppard, M.T. Holder, T.D. Loecke, P.C. Reid, J.D. Bever, and D.C. Reuman. 2020. Copulas and their potential for ecology. *Advances in Ecological Research* 62:409-468.

Kortessis, N. and P. Chesson. 2019. Germination variation facilitates the evolution of seed dormancy when coupled with seedling competition. *Theoretical Population Biology* 130:60-73.

Kortessis, N. and P. Chesson. 2021. Character displacement in the presence of multiple trait differences: Evolution of the storage effect in germination and growth. *Theoretical Population Biology* 140:54-66.

Roy M., R.D. Holt, and M. Barfield. 2005. Temporal autocorrelation can enhance the persistence and abundance of metapopulations comprised of coupled sinks. *The American Naturalist* 166:246-261.

Schreiber, S.J., A. Hening, and D.H. Nguyen. 2023. Coevolution of patch selection in stochastic environments. *The American Naturalist* 202:122-139.

Supplemental Material (not copyedited or formatted) for: Nicholas Kortessis, Gregory Glass, Andrew Gonzalez, Nick W. Ruktanonchai, Margaret W. Simon, Burton Singer, Robert D. Holt. 2025. "Metapopulations, the Inflationary Effect, and Consequences for Public Health."
The American Naturalist 205(3). DOI: https://doi.org/10.1086/733896.

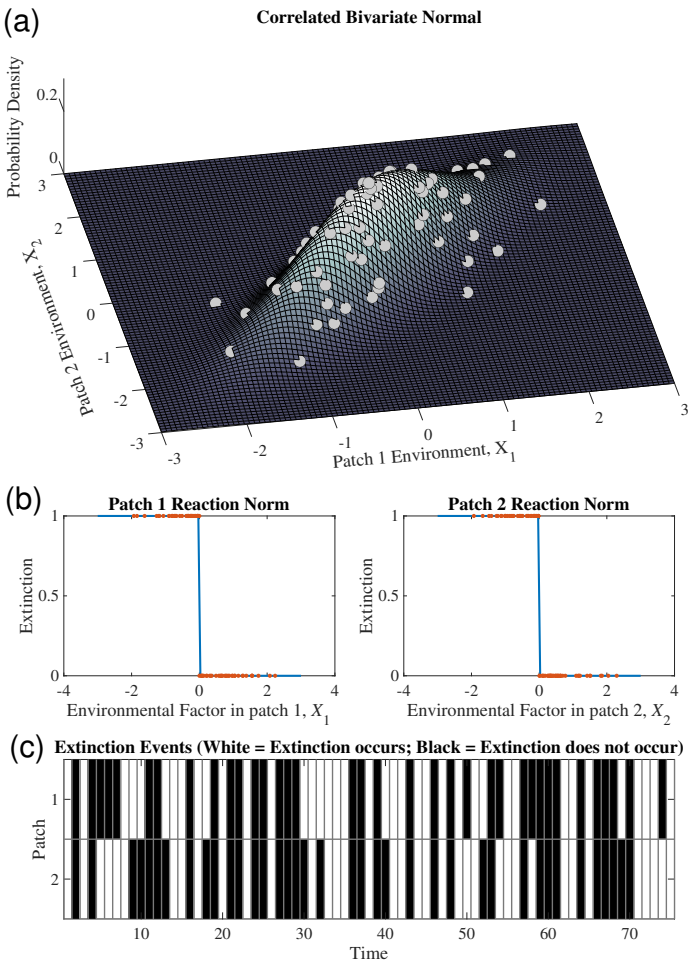

Figure S2: Example construction of correlated extinction events with two patches in the occupancy model. (a) The correlated probability distribution for $\mathbf{X}$ representing the two environmental factors present in the patches that affect extinction. Each marginal has mean 0 and unit variance, and the correlation between marginals is $\rho_E = 0.85$. The marginal variables can be considered as latent variables measuring habitat quality. Gray circles represent a random sample from this bivariate distribution. (b) The environmental factors are translated to extinction events in each patch. The relationship between $X_i(t)$ and the extinction event is given by (S18) with $e = 0.05$ and is shown by the blue line. The random sample in (a) is shown by the red points in (b). (c) The spatio-temporal pattern of extinction events from the random sample in (a) and transformed in (b). Because of the correlated nature of the environmental variables, extinction events are also correlated across space such that an extinction event in one patch means that extinction is likely in the other patch.

Supplemental Material (not copyedited or formatted) for: Nicholas Kortessis, Gregory Glass, Andrew Gonzalez, Nick W. Ruktanonchai, Margaret W. Simon, Burton Singer, Robert D. Holt. 2025. "Metapopulations, the Inflationary Effect, and Consequences for Public Health."
The American Naturalist 205(3). DOI: https://doi.org/10.1086/733896.

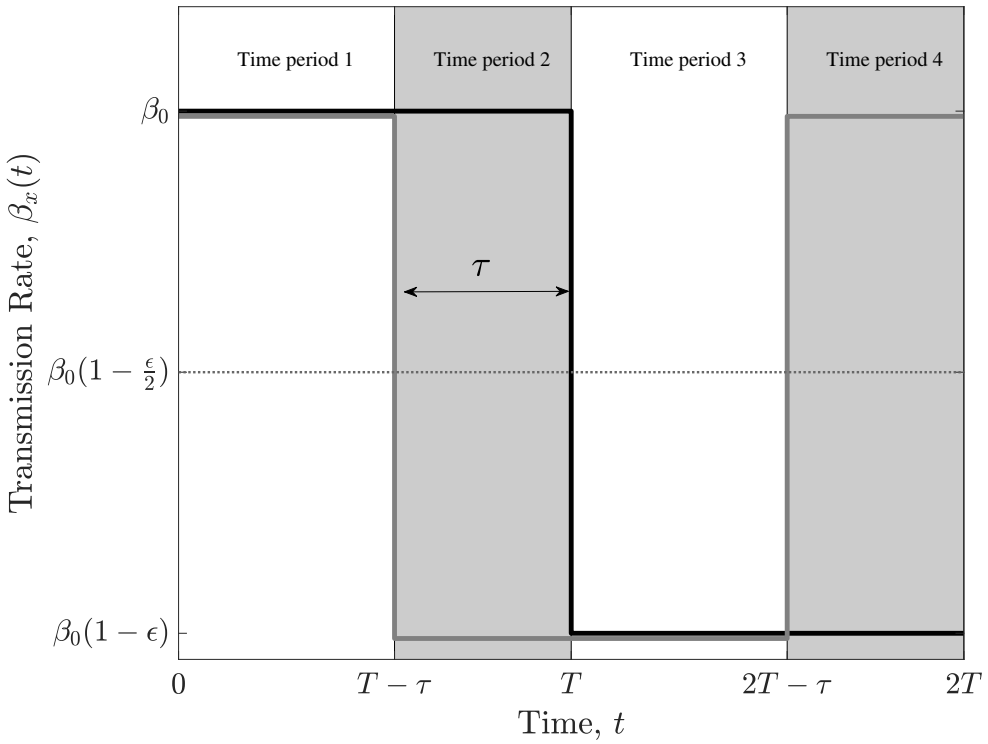

Figure S3: The square-wave function used to model differential timing of non-pharmaceutical interventions. The black line shows the transmission rate in the first patch and the gray line shows the transmission rate in the second patch. The dotted line shows the temporal average in each patch, $E_t[\beta(x,t)|x]$. Time can be partitioned into four distinct periods which fully describe the unique set of states the two patches can be in together.

Supplemental Material (not copyedited or formatted) for: Nicholas Kortessis, Gregory Glass, Andrew Gonzalez, Nick W. Ruktanonchai, Margaret W. Simon, Burton Singer, Robert D. Holt. 2025. "Metapopulations, the Inflationary Effect, and Consequences for Public Health."
The American Naturalist 205(3). DOI: https://doi.org/10.1086/733896.

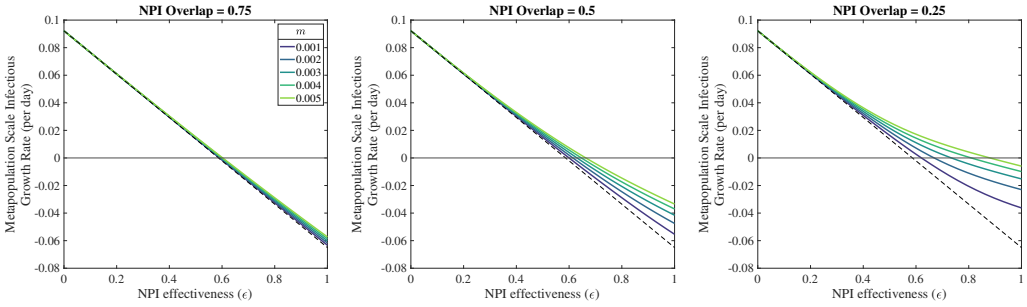

Figure S4: Metapopulation growth rate of the infectious class as a function of the effectiveness of an NPI.The dotted line shows the metapopulation spread of the disease assuming no spatio-temporal heterogeneity, which implies either coordinated NPIs or no movement. Actual spread rates lie above this line, reflecting that fact that the realized effectiveness of NPIs is diminished by asynchrony in the timing of NPIs. The difference between the dotted line any given solid line is the magnitude of the inflationary effect.

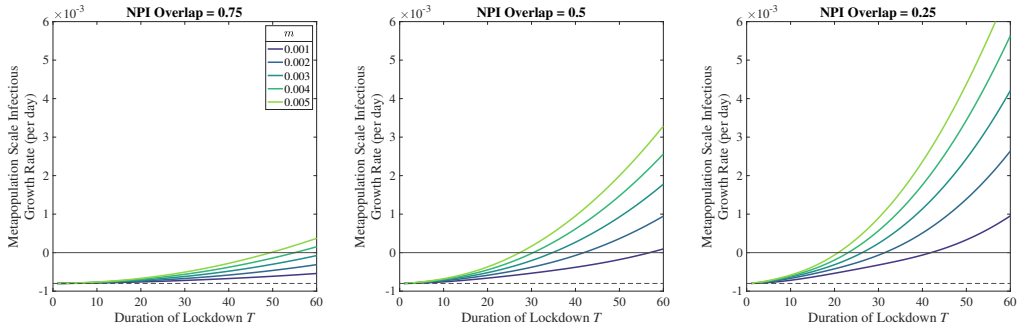

Figure S5: Metapopulation growth rate of the infectious class as a function of the duration of NPIs. Longer NPI application (and so longer durations of "business as usual") creates autocorrelated growth rates from the perspective of infectious hosts. As such, the inflationary effect is larger. The solid line gives the boundary growth rate above which the disease spreads in the metapopulation. The dashed line gives the baseline growth rate in the absence of any spatio-temporal variability in transmission.

Supplemental Material (not copyedited or formatted) for: Nicholas Kortessis, Gregory Glass, Andrew Gonzalez, Nick W. Ruktanonchai, Margaret W. Simon, Burton Singer, Robert D. Holt. 2025. "Metapopulations, the Inflationary Effect, and Consequences for Public Health."
The American Naturalist 205(3). DOI: https://doi.org/10.1086/733896.

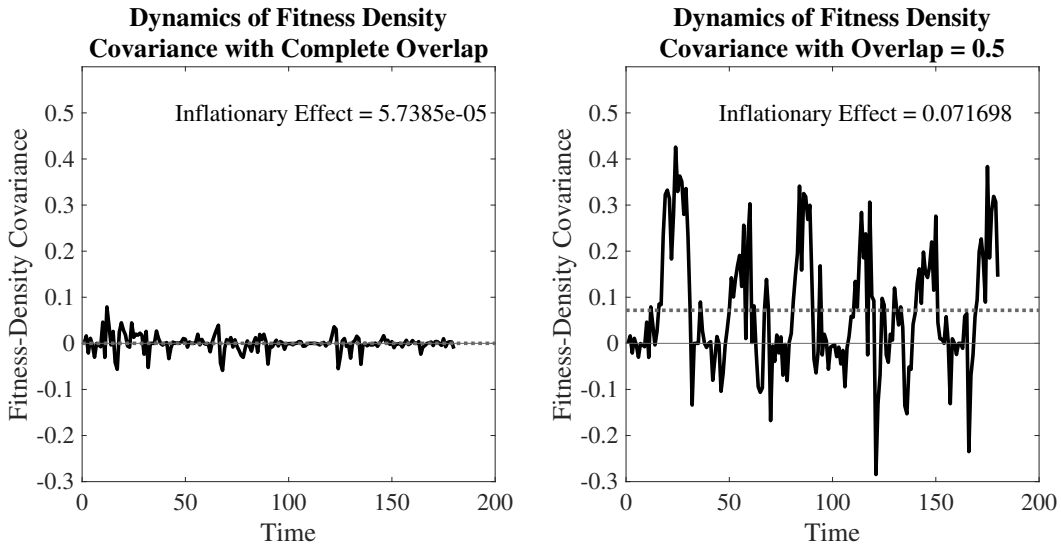

Figure S6: Mechanistic basis of the inflationary effect. Plotted are the dynamics of the fitness-density covariance for the stochastic SIR model simulated and presented in Figure 5b of the main text. The left panel shows the dynamics of the fitness-density covariance in the case with complete NPI overlap. Variability in the fitness-density covariance is caused by stochastic variation in the transmission rate. As such, it is zero over time on average (dotted line), meaning that the inflationary effect is zero by equation 4 of the main text. The right panel shows the same model with NPI overlap equal to 0.5. In that case, the fitness-density covariance gets to very large values, but only dips to small negative values. Averaging over time (dotted line) reveals a positive inflationary effect. Parameters identical to those in Figure 5b.